Design and Simulation of a MEMS Thermal Actuated Micropump

A Thesis submitted to the Department of Biomedical science & Engineering in fulfilment of the requirements for the degree of Master of Science in Biomedical Engineering

by

Shiangyu Lin (Student ID: 0854491)

Project Advisor: Dr. Prabir Patra

Project Advisor: Dr. Xingguo Xiong

UNIVERSITY OF BRIDGEPORT, CT, USA
SCHOOL OF ENGINEERING
DEPARTMENT OF BIOMEDICAL SCIENCE & ENGINEERING

ABSTRACT

In recently years, micromachining technology and biomedical are integrating with each other has provided us great convenient on many applications such as gene chip, drug delivery, nucleic acid synthesis etc. How to efficient and rapid transportation of microfluids has been a challenging for biomedical technology; follow by the rapid development of Micro-Electro-Mechanical – Systems and biomedical engineering. . United States of America has become one of the most potential technologies due to the demand of the medical examination and test increase step by step. But In nowadays, some of countries still used large traditional machine for medical tests, it may be a hindrance for obtain bio-information. If BioMEMS [1] technology used more widely, have very positive consequences as a whole. And less required sample for diagnostics, as well as lower reagents costs. Faster response times and process control due to short diffusion distances. It also can be safer platform for biological studies because of integration of functionality, smaller fluid volumes and energies. Another advantage is that lower fabrication costs, easier mass production and allowing cheap disposable chips. Thus, develop low costs devices with stable performance and portability and was able to meet the need of medical detection is the most urgent task. How fast and effective delivery fluid can be challenging in MEMS technology. Many research of micropump micropump [2] [3] have been published one after another. Such like Electro osmotic micropumps, piezoelectric micropumps, Pneumatic micropumps, Magnetic micropumps…etc. Pneumatic [4] is the one of surest and quickest method. In this poster, the design and simulation of a MEMS thermal actuated micropump is reported. The micropump consists of a microfludic chamber on top of a thermal actuation chamber. The PDMS (Polydimethysioxane) membranes [5] are activated pneumatically by air pressure which generates a rapid transporting of microfluids to target. The working principle of the micropump is analyzed in detail. Based on the theoretical analysis, a set of optimized design parameters of the micropump are suggested. Simulation is used to verify the function of the micropump. Compared to traditional methods, this MEMS thermal actuated micropump has some advantages [6], like low costs, more easy mass production. If integrate with testing chip...etc. It could provide a useful tool for biomedical field and be crucial for micro total analysis system. .

Bio-chip is kinds of modern high-tech chip. It integrate laboratory's functions on miniature chip that usually made by silicon chips and glass. It can be divided into two groups. That are "lab on a chip" and" Micro array". Microfluidics technology is a very important part of bio-chip. In micro scale, surface area volume ratio and forces within the Atom increase because tiny size and geometry. In this situation, fluid resistances also increase in micro channel. Thus, driving force is necessary for fluid acting in micro channel. It is one of the motivations. Another goal is formulate a micro pump that has the advantages of convenient arrangement

and usage, time saving, and material saving; in order to reduce the cost and consider the possibility of disposable chip. This paper used the Polydimethylsiloxane for basic materials. They have some advantages like high biocompatibility, high light transmission and producing simple.

Keywords: (Microelectromechanical Systems (MEMS), micropump, ANSYS simulation

TABLE OF CONTENTS

LIST OF TABLES

LIST OF FIGURES

FIGURE

NOTATION

T	temperature
d	duty ratio
τ	pump period
R	resistance
Cp	heat capacity
U	voltage
ΔH	enthalpy
P	Pressure
V	air volume
L	chamber radius
a	radius of the specimen
D	plate rigidity
E	Young's modulus E

h	plate thickness
Nx, Ny	normal forces per unit length
Nxy, Nyx	shear forces per unit length
q	load intensity
r	radius of a given position
u	radial displacement
x, y, z	3D coordinates
∂	partial differentiation
ŋ	plate deflection
	maximum plate deformation
v	Poisson's ratio

Chapter I Introduction

Micropump is a MEMS technology of special interest in micro fluidic research, and has become available for industrial product integration in recent years. Micropumps were started in middle 1970s. Before 1990s, mechanical pumps were mainly studied. After 1990s, non-mechanical pumps were introduced. Their miniaturized overall size, potential cost and improved dosing. One of the first documents about micro pump was presented by Thomas and Bessman in 1975. It contain muti piezoelectric disc benders combine with solenoid valve and pumping chamber. It was designing for implantation for human body. 1984 Smits was patented the silicon micro fabrication technologies. Few years later, he published the peristaltic pump in 1990. This pump consists of three piezoelectric discs and purpose was for his insulin delivery systems. In this chapter we are brief overview of a variety of micropumps and their applications. The review will present key features of micropumps such as actuation methods, working principles, construction, performance parameters and their medical applications.

In general, micropumps can roughly be divided into two groups: One called "mechanical" micro pump. The micro pump that have moving mechanical parts such as pumping diaphragm and check valves that use the oscillatory or rotational forces to control micro fluid. The most popular mechanical micropumps such like electrostatic, piezoelectric, shape memory alloy (SMA), bimetallic, ionic conductive polymer film (ICPF), electromagnetic and phase change type.

Another one is non mechanical micropump. Non mechanical type of micropump has to transform certain available non-mechanical force into kinetic momentum so that the fluid in micro channels can be driven. This type often consists of two check valves and a chamber with movable membrane. By some mechanisms, membrane can be actuated to change the volume of chamber. Non-mechanical micropumps include magneto hydrodynamic (MHD), electro hydrodynamic (EHD), electro osmotic, electro wetting, bubble type, flexural planar wave (FPW), electrochemical and evaporation based micropump.

Based on these two types can be further subdivided into several subtypes. Here lists some most common types of micropump:

mechanical micropumps:

1.1 Phase change type micropump

The working principle of phase change type micro pump is based on morphologic changed of fluid. This type of micro pump used to have a fluid chamber, heater and membrane. The basic structure shown in Fig 1-1.

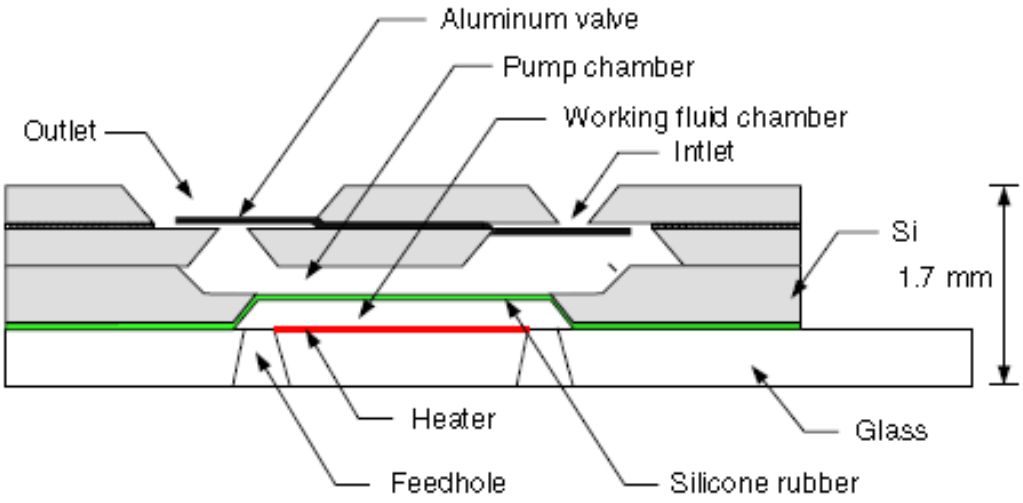

Figure 1-1 Phase change type micropump

The actuator in phase change type of micropumps basic composed by a heater, a diaphragm and a working fluid chamber.

In 2003, Sim et al. [7] reported a paper "A phase change type of micropump with aluminum flap valves". According to this paper, this micropump used silicon for the membrane material. Materials of substrate are silicon and glass. The actuator combined membrane, two substrate and micro heater. The working principle is based on vaporization and condensation of the working fluid. When it applied voltage to micropump, the working fluid become vapour that increase air pressure inside the chamber and push the membrane deflection. When it cut off the voltage, silicon membrane restored shape because working fluid condensation and pressure cold down. The maximum flow rate of the micropump was 6.1 μl/min when it applied voltage 10V at 0.5 Hz. The maximum deflection appeared on the air pressure raised to 68.9 kPa.

1.2 Rotary micropump

Rotary micropump commonly use magnetically driven. Magnetic stator and central pin is perm alloy. Rotors were separately made and assembled into pump by hand. The flow rate depended on speed of rotor spin. Pumping speeds increased when pressure ratings go up and the volumetric capacities decrease. The relationship can be expressed as :

$$Vd = q\ V\ 1N$$

Where N is the rotor rotates rate (rpm), q is the total trap number exist at the rotor, V1 is the volume of fluid. If the torque generated from motor keeping pump in a

constant value , we may able to calculate the developed pressure by following equation

$$P_a = C\frac{T_q N}{V_d}$$

C is the constant here, Tq as the motor torque. This type of pump without diaphragm but they are the complex fabrication process and reliability. Another concern is the wear resistance.

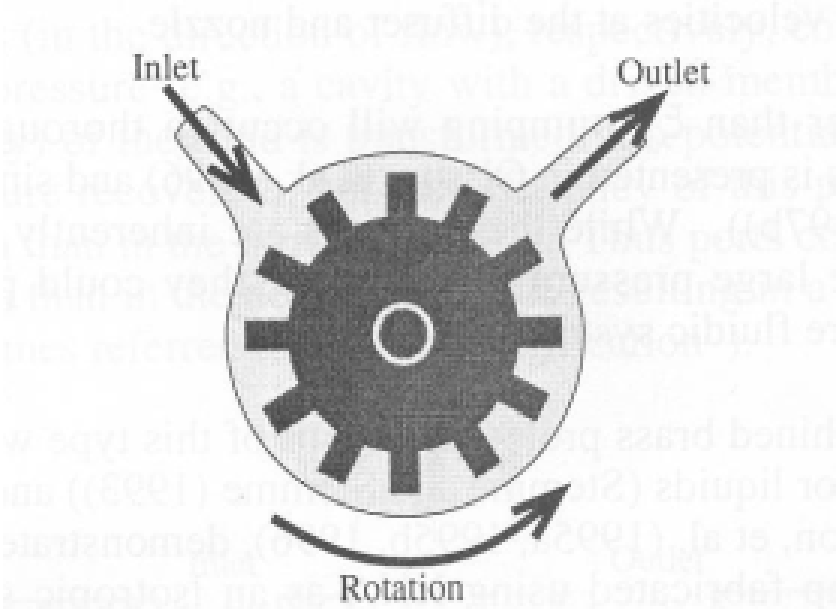

Figure 1-2 rotary micropump

Chong H et al [8] reported a rotary magnetic actuators micropump in 1995.The maximum flow rate are 24 μl/min when the rotor speed reach to 5000rpm. Driving voltage around 3v, power consumption was around 0.5w. The main materials of this micro pump are poly silicon and silicon.

1. 3 Piezoelectric micropump

The piezoelectric micropump is actuated by the deformation of the piezoelectric materials. In typically, it consists of a piezoelectric disk attached on a diaphragm, a pumping chamber and valves. Piezoelectric pumping: use piezoelectric actuation for driving mode. It also used the suck and push forces by change the piezo actuator shape. It has some goodness like large actuation force, short response time and simple structure. The weakness is low working frequency, difficult to fabrication, small stroke and high actuation voltage.

Van Lintel, S. Bouwstra et al. Reported a first piezoelectric micropump in 1988

[9]. It is a reciprocating displacement type micropump that consists of a pump chamber, a thin glass pump membrane actuated by piezoelectric plate and passive silicon valves to direct the flow. It was using cyano acrylate adhesive for fixed piezoelectric plate. It was the first reported work on a successfully fabricated micropump using micro machining technologies.

2005, K. Junwu, Y. Zhigang, P. Taijiang..et al. Published a paper "Design and test of a high performance piezoelectric micropump for drug delivery"[10]. It is a high performance piezoelectrically actuated cantilever valve micropump. It has a cantilever valves for improved the output values. The flow rate of the micropump are 3000 and 3500μl/min with back pressure of 9 kPa and 27 kPa that depend on the different size of cantilever valves. The micropump use conventional technology for fabrication. The pump consisted of muti stacked layers, bronze membrane with PDMSs body and cover. A maximum back pressure of 27 kPa achieved by the micropump was higher than the normal blood pressure of 15 kPa. Therefore the micropump design was applicable for drug delivery.

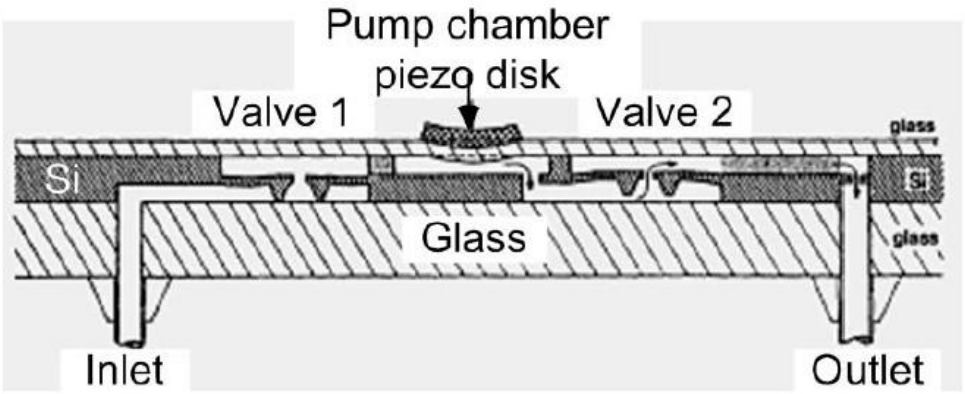

Figure 1-3 Piezoelectric microump [11]

1. 4 Shape memory alloy micropump

This type of micropump contain sharp memory alloy. Shape memory alloys are special alloys such as Au/Cu, In/Ti, and Ni/Ti. The most common one is Nickel titanium. According to the sharp memory effect, material membrane can be divided by two solid phases. One is called austenite phase and another is called martensite phase, both of them manipulated by temperature. Austenite is much harder than martensite when it in high temperature and martensite is much more ductile than austenite when it in low temperature. Martensite materials can undergo the larger deformation. Shape memory alloy used these two phase for actuation.. The temperature can be precisely generated by an electrical current. Large pumping rate, high working pressure are their advantages. Disadvantage such like low driving

frequency, high power consumption. The membrane od SMA micropumps is commonly made by titanium nickel alloy (TiNi) because it is high pressure, restoring force and pumping rate. High work output per unit volume makes it suitable in sizes for MEMS applications.

The first shape memory alloy micro pump was presented in 1997 by Benard et al.[12] Two titanium nickel plates was for reciprocating motion. Two plates actuated by alternating heat. When it applied heat on titanium nickel plates, the shape became bent down. According this paper, the maximum flow rate was 49μl/min when it applied 0.9A current. The operating frequency was 0.9Hz, back pressure of 4.23 kPa and voltage was 6V.

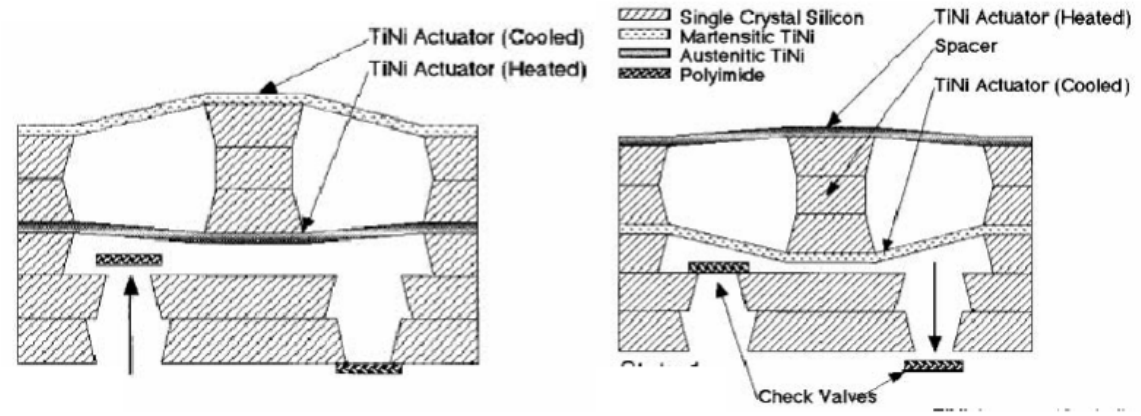

Figure 1-4 Shape memory alloy micropump [13]

1. 5 Electrostatic micropump

The first electrostatic micropump was presented in 1991 by J.W. Judy, T. Tamagawa []4]. The micropump consisted of an active check valve, a pumping membrane and an active outlet valve. Above of all were sealed inside by silicon nitride and were actuated by electrostatic force. Actuation voltages of approximately 50V were required for valve closure and membrane deflection, but no record about pumping action of it.

Teymoori and Sani reported a design and simulation of an electrostatic peristaltic micropump for drug delivery applications in 2005 [15]. According to this report, the pump size was 7 mm × 4 mm × 1 mm. The flow rate was approximate to 9.1μl/min and driving voltage was 18.5V. It was suitable for drug delivery applications such as chemotherapy. The micropump was designed for drug delivery requirements such as drug compatibility, flow rate controllability and low power consumption and shrinks the bio chip size.

Electrostatic micro pump use electrostatic force for pumping that based on Coulomb's law. Coulomb attraction force between oppositely two charged plates. The force can be expressed as

$$F = \frac{dW}{dx} = \frac{1}{2} * \varepsilon 0 \varepsilon r A V 2 / x^2$$

Where F is the electrostatic actuation force, W *is* energy stored, ε (=$\varepsilon 0 \varepsilon r$) the dielectric constant, A is electrode area, V is power and x is the electrode spacing. In this type, membrane is deformed in either direction as voltage is applied on the two opposite electrostatic plates. The two opposite electrostatic plates located show in Fig 1-6. When it remove the voltage, membrane flat again. The advantages of electrostatic micropumps are low power consumption, simply structure, good control of actuation and short response time. The weaknesses are high actuation voltage and small stroke. The maximum deflection is around 5 μm when it applied 200 voltages.

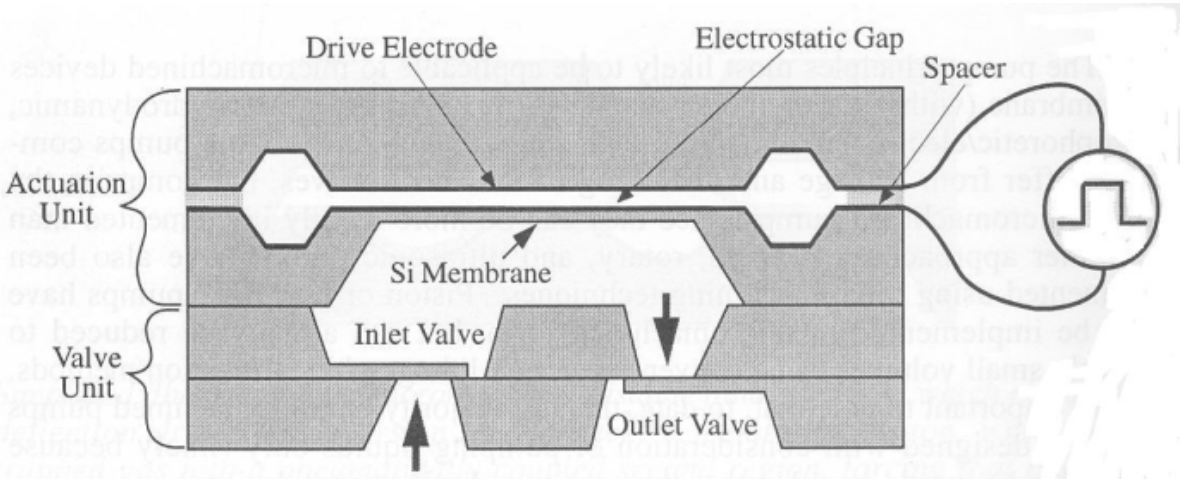

Figure 1-5 Electrostatic microump [16]

1. 6 Bimetallic micropump

Zhan et al. publish the first silicon based bimetallic micropump at 1996 [17]. The diaphragm was made by silicon substrate with the thin film aluminum. The body size was 6mm×6mm×1 mm. The flow rate was 45μl/min, back pressure was12 kPa. Driving voltage and frequency were 5.5V and 0.5 Hz .

The structure is similar to shape memory alloy or other mechanical micro pump, but the actuations way are different Fig1-7**.** The basic theory of this type pump is quite simply. Different materials have difference of thermal expansion coefficients. Bonded materials together and applied heats on it, the thermal stress are induced to

force it changing shape. The main advantage of bimetallic micro pump is low energy consumption compared to other types of micro pump. The main disadvantage is low deformation of membrane because of the thermal expansion coefficients.

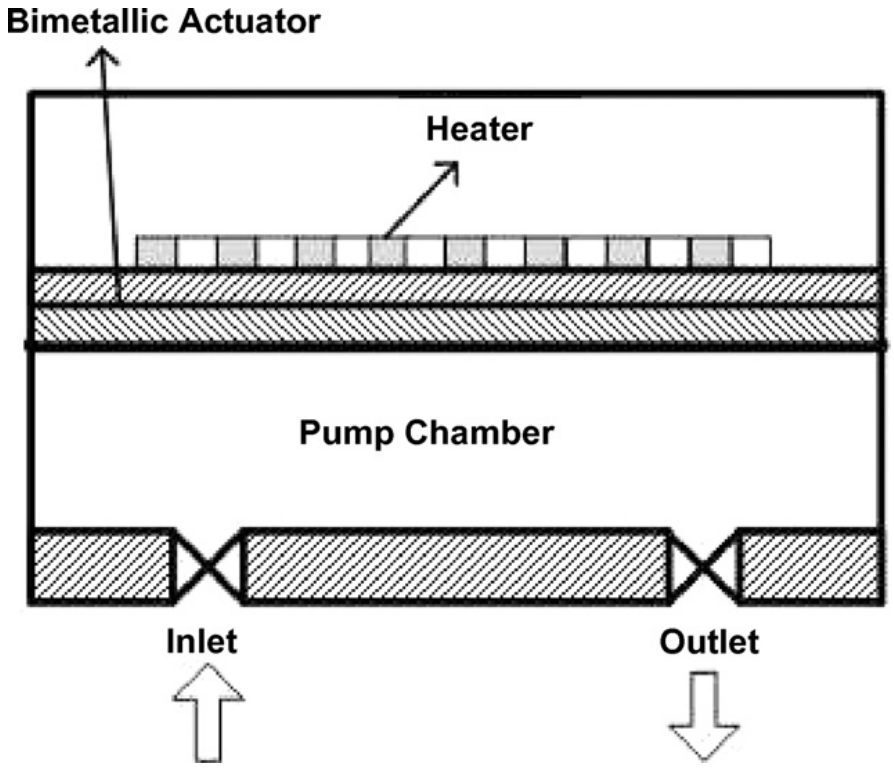

Figure 1-6 Bimetallic microump

The actuation plate was made by two different metals that can become different degrees of deformation during heating. The deflection of a diaphragm, made of bimetallic materials, Is achieved by thermal alternation because the two chosen materials possess different thermal expansion coefficients.

1.7 Electromagnetic micropump

In typically, electromagnetic micro pump consists of a permanent magnet, a set of drive coils chamber, inlet valves, outlet valves and diaphragm. Magnet or the set of coils may be attached to the membrane. It is shown in Fig 1-7.

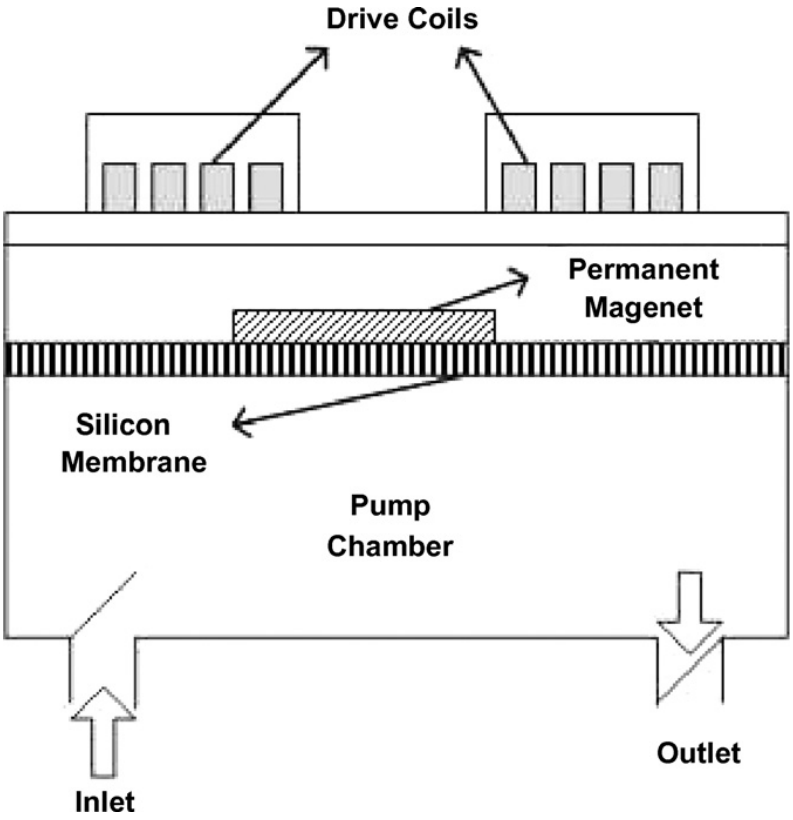

Figure 1-7 Electromagnetic micro pump

Electromagnetic micro pump actuated by magnetic field with currents. The theory based on Lorentz force. The Lorentz force can be presented like below:

$$F = (I \times B)L \quad (9)$$

In here F is the Lorentz force, I *as* current, B *is* the magnetic field and L is the length of wire. When it applied current through the coils, the resulting magnetic field creates an attraction or repulsion between the coils and the permanent magnet. It is the basic working principle of electromagnetic micro pump. Compare with other actuation ways, electromagnetic actuation provides excellent actuation force with low energy usage. The main drawback is difficult to reduce size because magnetic materials has limit to fabrication.

In 1999, Bohm et al published a paper "A plastic micro pump constructed with conventional techniques and materials". [18] It is the first micro pump that used magnetic force for actuation. The membrane of micro pump combination with permanent magnet and coil was placed on the body top. The inlet and outlet valves were placed on the bottom side of the body. Despite the body of micro pump was not small enough (10mm×10mm×8 mm) because of fabrication reason. It still had high flow rate (40,000μl/min in air and 2100 μl/min in water) and good energy consumption (0.5W).

Non-mechanical micropumps

Since the early 1990s, many non-mechanical micropumps have been reported. Non-mechanical micropumps require to transform of non-mechanical energy to kinetic energy, such like magnetohydrodynamic, electrochemical..etc. Compare with mechanical micropumps, non mechanical micropumps has some advantages such like more easy to design or fabrication because no mechanical moving parts.

1.8 Electroosmotic micropump

Electro osmotic pump (EOP), is pumping flow by use an electric field. It is basic on electrokinetic phenomenon. The working principle is generated by an external electric field applied on an electric double layer (EDL), generates high pressures and high flow. The ionic fluid moves by stationary,. When ionic solution through and contact to solid surface, the electrical charge is adhered on the solid surface because negatively charged surface attracts the positively charged ions of the solution.

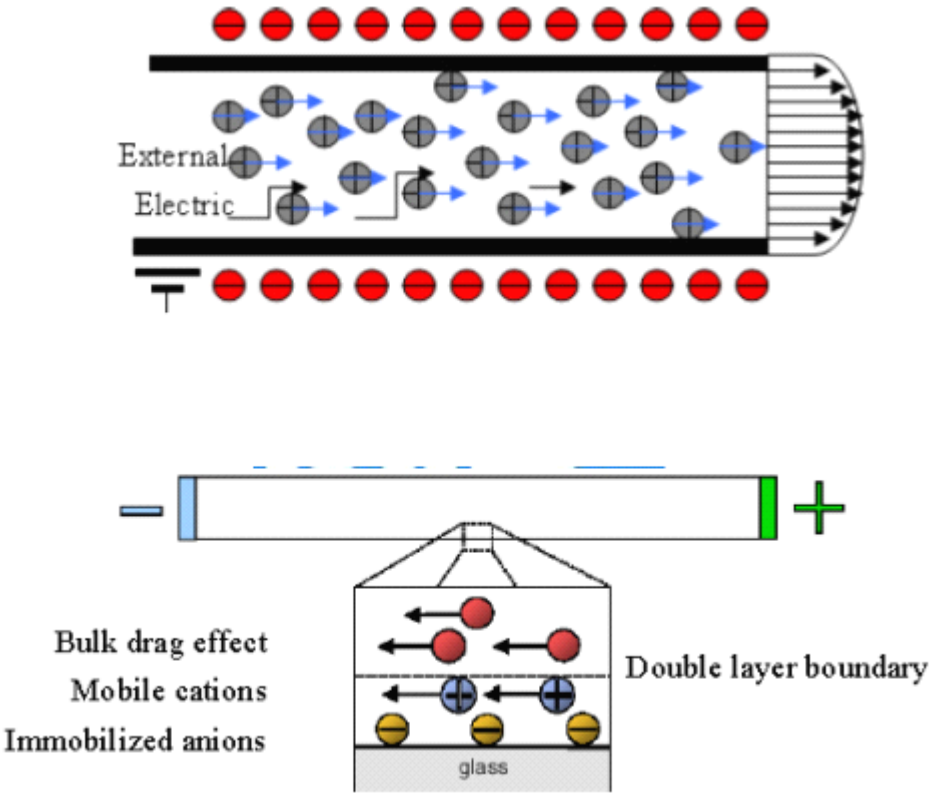

Figure 1-9 Electroosmotic micropump [19]

2001, Zeng et al [20] published a paper "Fabrication and characterization of electroosmotic micropumps". According to this paper, silica was the main material of this pump. The maximum were approach 3.6 µl/min when it applied 2kV voltage. This type of pump have no moving parts such like valves , membrane. That more durable than other type pump which contain moving parts. It is also quite when it operate. The major limitations are high energy consumption.

1.9 Diffuser micropump

The working principle of diffuser pump is based on suction force and push force when membrane bent down or bent up. Diffuser is a channel with a increasing cross –sectional area and the shape usually like conical or rectangular. The main functions of diffuser is to transfer kinetic energy to pressure, i.e suction force When fluid flows in one way or the other, it will encounter different flow resistances caused by the diffuser and it is similar with membrane pump.

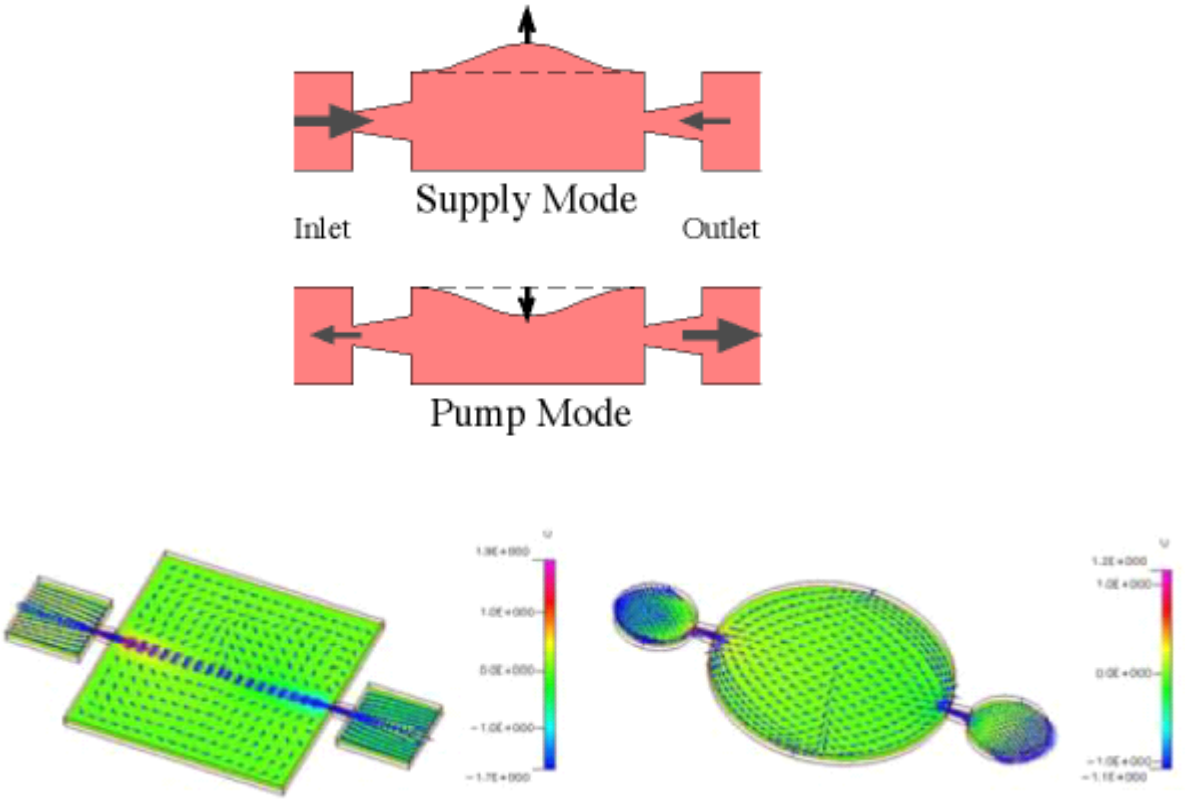

Figure 1-9 Diffuser micropump

In 1993, The world first diffuser pump reported by E. Stemme and G. Stemme. [21] The idea was that used diffuser elements instead flow control parts. The advantages are simple fabrication, free of valve fatigue. Weakness are sensitive to bubbles, low operating pressure.

1.10 Electro-wetting micropump

Electrowetting micro pump is modify the wetting abilities by applied voltage for pumping. The term electrowetting was first appeared on 1981, but this ability was explained by Gabriel Lippmann in 1875. Electro wetting ability related to surface tension. The electrolyte contact angle changed due to applied voltage. Continuous electro wetting can use for pumping by control the surface tension between two immiscible solutions. The most common material for electro wetting are mercury. If we put mercury into electrolyte solution and also put electrodes on both side. When it applied voltage, the interface of mercury will charge electric potential. The electric potential are not equal of each side because of protonation effect on mercury surface. The different surface tension push mercury move from high electric potential to low electric potential.

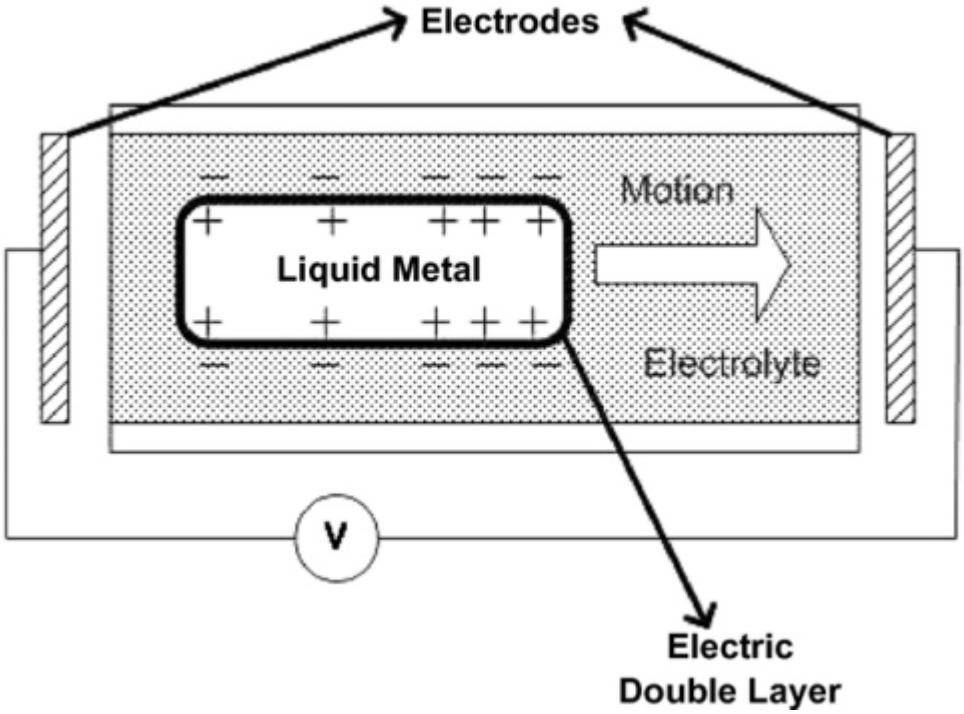

Figure 1-10 Electro wetting micropump

In 2002, Yun et al. [22] reported a micropump by used continuous electro wetting actuation. The micropump consisted of three plates stack together. Micro channels combined electrolyte and glass wafer. The membrane deformation by mercury drop pushed electrolyte. The maximum flow rate was 70 μl/min. It appeared when it applied 2.3 voltage. The power consumption for this design was approximate 170 W. The maximum air pressure can reached to 0.8kPa with 25Hz frequency. In typically, electro wetting micro pump have some strengths such like quick response time and low power consumption.

Chapter II Micropump design

2.1 working principle

The structure design of the MEMS thermal micropump is shown in Figure 2-1. The figure shows that a cylindrical pump container is connected to an inlet and outlet ports. There are embedded valves at the entrance of the inlet/outlet to regulate the flow direction of the microfluid [23] [24]. The microfluid is only allowed to enter the container via inlet, and come out of the container via outlet. The reverse microfluid flow is forbidden by the valves (figure 2-2). In the middle of the pump body, there is an elastic membrane, which can bend under pressure difference from its top and bottom surfaces. The edge of the elastic membrane is connected to the inner sidewall of the pump chamber. The top Si cover seals the chamber, and Al thermal resistor [25] is deposited on the bottom surface of the top cover. A certain amount of air is sealed inside the air chamber.

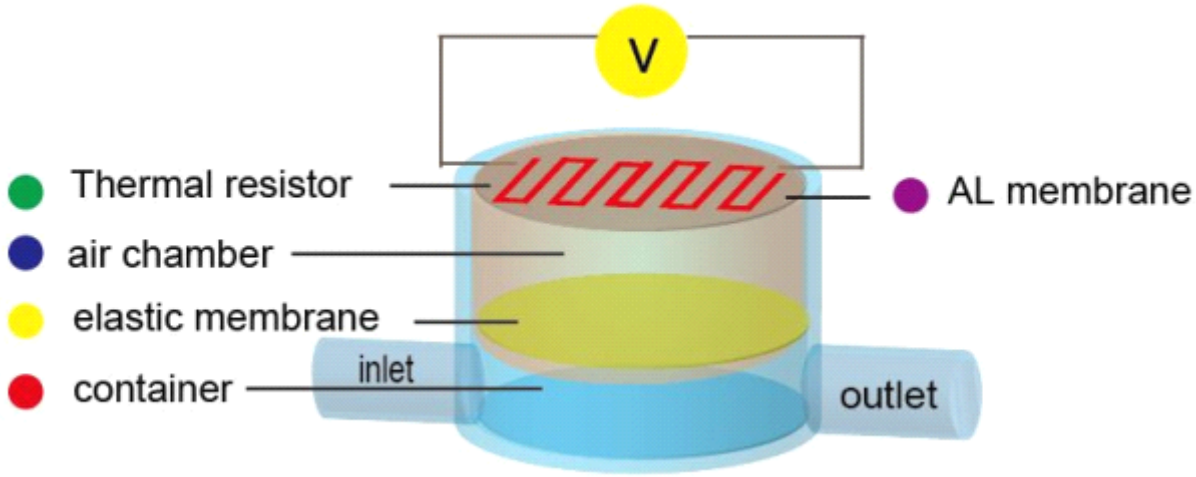

Figure2-1a .Structure of micropump

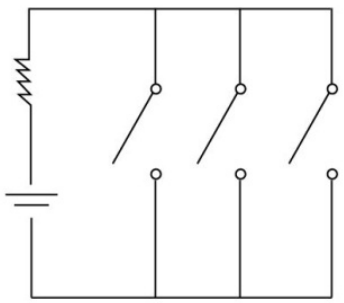

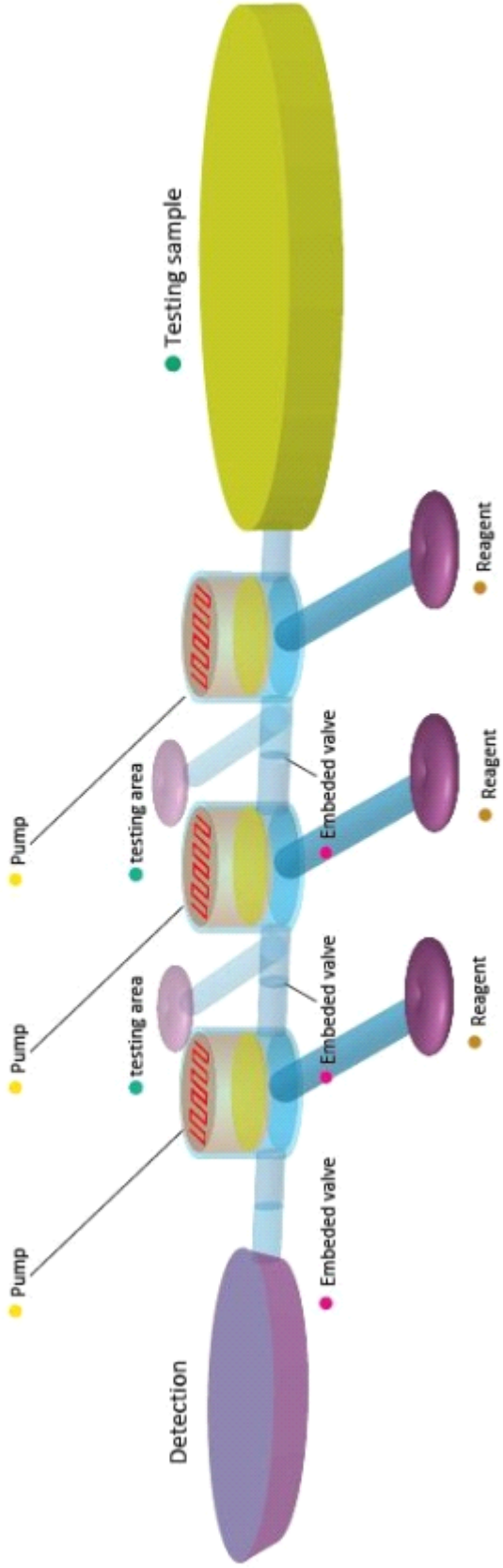

Figure2-1b .overiw of micropump

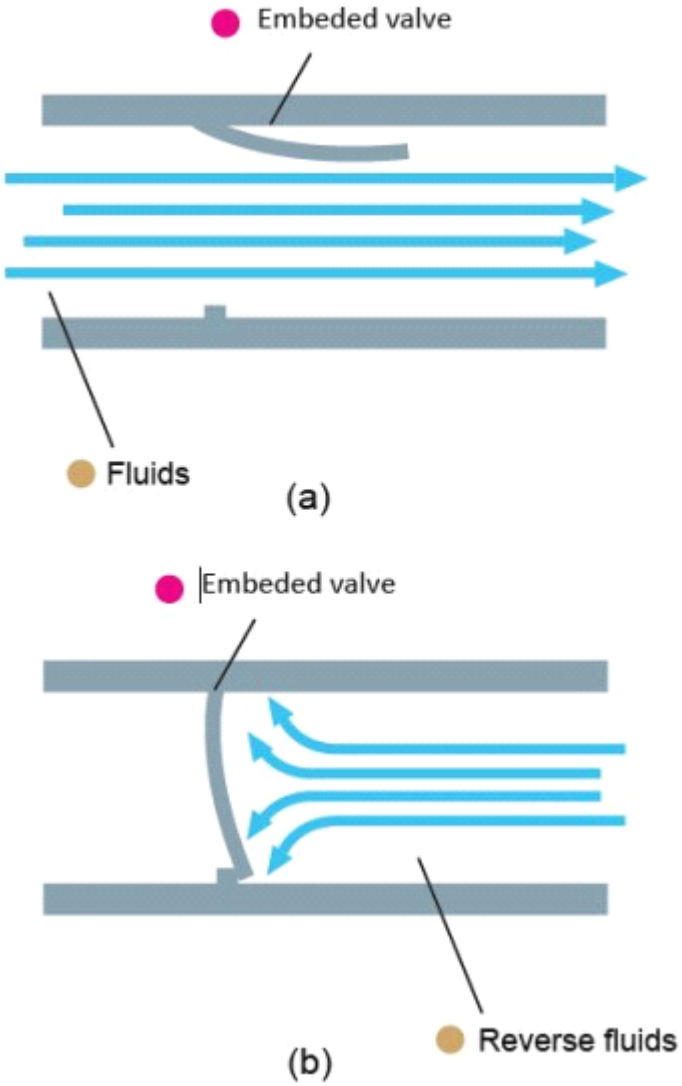

Figure 2-2 Cross section view of in/outlet tube:
(a) Embedded valves just allow flow in one direction. When the pump work, fluids through the tube and valve open. (b) The reverse fluidics is forbidden by the valves

When a voltage is applied to the thermal resistor, conducting current results in Joule heat and heat up the temperature of the air chamber. As a result, the air expands and pushes the elastic membrane [26] to bend down. The volume of chamber container is reduced and the microfluid inside the chamber is pumped out via outlet. However, if the driving voltage is disconnected, the air temperature inside the air chamber will decrease due to thermal dissipation. Thus the volume of air shrinks, and the elastic membrane returns to its flat shape (Figure2-3). As a result, the volume of container expands, and the microfluid is sucked into the pump. By repeating this process (applying a pulse voltage), the microfluid can be continuously pumped in from the inlet and pumped out from the outlet (Figure2-4).. This is the working principle of the micropump.

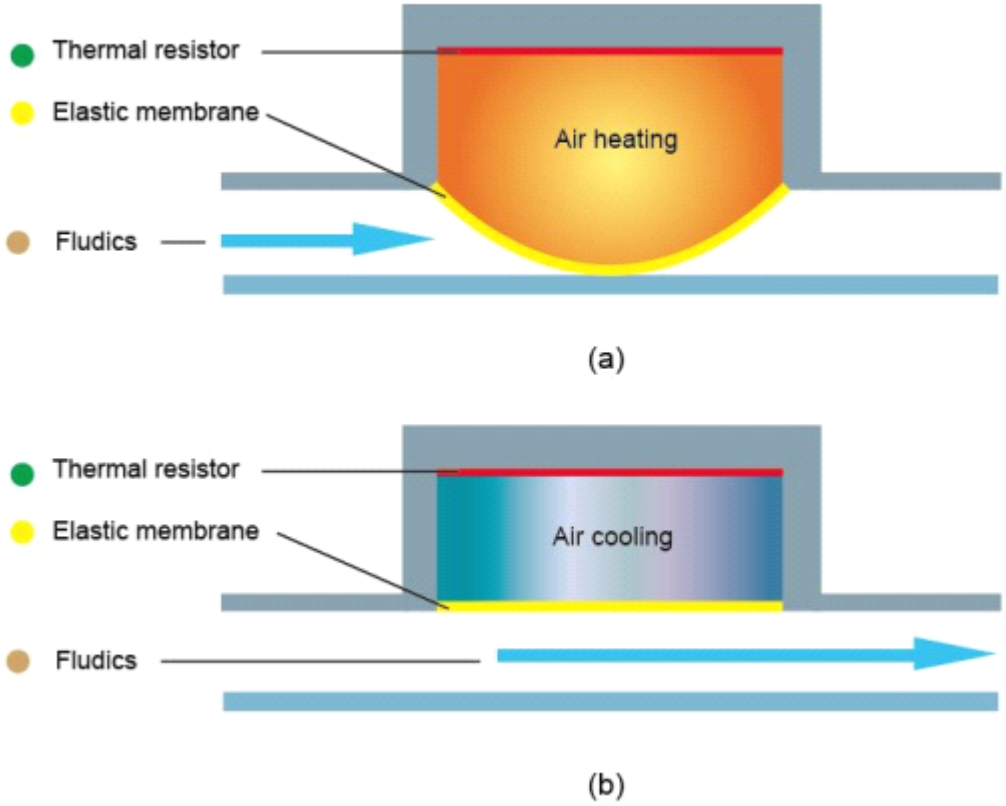

Figure 2-3 Schematic of thermal actuated micropump:
(a) The air in the chamber expands when heated. Elastic membrane bends down.
(b) Removal voltage, air cools down. Membrane become flat again

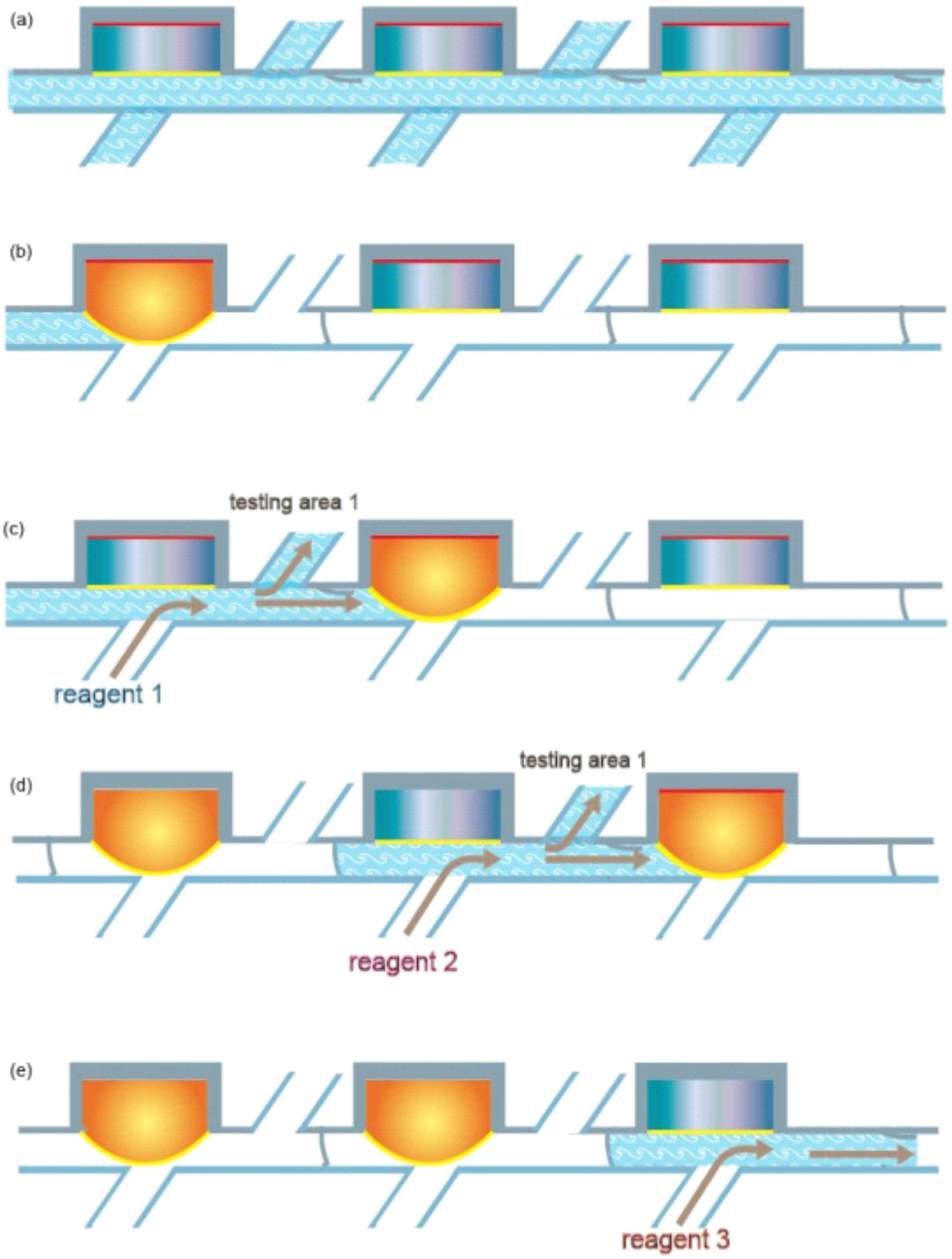

Figure 2-4: sequential diagram of thermal actuated micropump:

(a) All pumps open. The sample can directly through all channels to detection. (b) Close the first pump and stop the sample to next section. (c) Open the first pump. The reagent 1 flow into main channel and mix sample fluid. Two mixed fluids stopped by second pump and It can moves quickly away out to testing area 1. (d) Like step (c), the flow keep moving to next section and stopped by third

pump. Reversed *fluid will not flow back because the embedded valve. (e) Repeting the previous steps, the sample and three reagents mixed*

2.2 Control system

In this experiment, it is quite easy to use Heating device for this micropump. Connect power to heating resistor and cover an aluminum plate embedded in top of air chamber. To choose aluminum plate is because of the higher surface heat transfer area.

The estimate heating resistor dimension formula [27] is like below (2-1)

(2-2.1)

R	= Resistance	Ω
ρ	= Electrical resistivity	Ω·m
l	= Cable length	m
A	= Cross-sectional area	m2

The value of the electrical conductivity (conductance) and the specific electrical resistivity is a temperature dependent material constant. Mostly it is given at 20 or 25°C.

Resistance $R = \rho \times (l / A)$ or $R = l / (\sigma \times A)$ (2-2.2)

The table 2.2 shows the specific electrical resistivity of different materials. Electrical is commonly represented by the letter ρ (rho) and electrical conductivity is represented by the Greek letter σ (sigma). Consider the economic situation and efficiency. Copper resistor combines of the two.

Electrical Conductors	Electrical conductivity	Electrical Resistivity
Silver	σ= 62	ρ= 0.0161
Copper	σ= 58	ρ = 0.0172
Aluminum	σ= 36	ρ = 0.0277

Table 2.1 Comparison with difference materials

We can also calculate the resistive heating by using the following equations (2-2.3.) Thus, we knew the enthalpy from heating resistor and consumption of power.

- $\Delta H = mC_p\Delta T$
- $\Delta H=\int(Pwr)dt$ (2-2.3)

Assume voltage pulse V is applied to heating resistor R for a time period of T, the generated Joule heat by the heating resistor is:

$Pwr=U^2/R$

$\Delta H=\int(Pwr)dt=PwrT|^T_0$

$$E = (V^2 / R) \cdot T \tag{2-2.4}$$

Where R is the resistance of heating resistor. Assume there are N folds of heating resistor, and the width, length and thickness of each fold is w, l and t respectively,

$$R = N\rho l/(wt) \tag{2-2.5}$$

We assume that the energy is transferred efficiently from heating resistors to the air inside the chamber as η ($0<\eta<1$ due to heat dissipation. Hence the resulted temperature increase of the air due to thermal heating is:

$$\Delta T = \eta E/(m_{air} \cdot c_{air}) \tag{2-2.6}$$

Where m_{air} is the mass of air, and c_{air} is the heat capacity of air.

2.3 Air expansion

In this device, the main function of sealed air inside the actuation chamber is that expansion size for bend down the PDMS membrane. In this part we can use gas law [28] for assumption. (2-3.1). the sealed air inside the chamber follows combined gas law:

$$P_2 = \left(\frac{\Delta T + T_1}{\Delta V + V_1}\right)\frac{P_1V_1}{T_1} \tag{2-3.1}$$

$$P_1V_1 / T_1 = P_2V_2 / T_2$$

where P_1 is the initial air pressure before heating (P_1=1atm), V_1 is the initial air volume ($V_1=S\times h_1$, where S and h_1 are the cross section area and height of air chamber), T_1 is room temperature (T_1=27ºC=300K), P_2 is the final air pressure inside the chamber, V_2 is the final air volume after thermal expansion, and F is the final temperature of air.

2.4 Membrane deflection:

Bending of plate base is complex. There are changes in mechanical properties of the fabric such as weight, thickness, stiffness, permeability, or breaking strength and elongation. [29] . Thus, simplified deflection calculations are required. In order to understand the relationship between stress and deformation of membrane. This research was made to analyze membrane deflection by applying Kirchhoff-Love theory of plates (classical plate theory) [30] and The Mindlin-Reissner theory of plates (first-order shear plate theory [31]).

2.4-1 Kirchhoff–Love theory

The Kirchhoff–Love theory (1888) of plates is an extension of Euler-Bernoulli beam theory and used to determine the stresses and deflections in thin plates subjected to forces and moments.

Love Kirchhoff assumptions [32]:

1. The thickness of membrane (d) has to much smaller than smallest bending radius.
2. Straight lines normal to the mid-surface remain straight after deformation
3. Straight lines normal to the mid-surface remain normal to the mid-surface after deformation
4. The thickness of the plate does not change during a deformation.

2.4-2. Classical shell theory and first- order shear deformation theory

The scholar soon later modify their Kirchhoff-Love theory and with appropriate attitude. The first one is called Classical shell theory (CST) [33]. This is based on Kirchhoff–Love theory but discard the influence of transverse shear force. This theory applies for very thin plate (h/r) < 1/80. It simplifies the calculation of the plate deformation.

The second one is First- order shear deformation Theory (FSDT) [34]. Unlike Classical shell theory, transverse shear force factors are taken into account. It can apply for plate that thickness ratio under 1/20 and with good results. Most size of membranes is under this range. Therefore, it is widely used for analysis membrane structure.

The geometric nonlinear can be expressed as the strain effect of the neutral plane of a membrane when the deflection of membrane larger than its thickness. When the deformation is small, the membrane can be seen as pure bending by the lateral loading.

Consider the equilibrium of a small element cut from the plate with two pairs of planes parallel to the xz and yz planes. Assume there has a force acting on the middle plane of the membrane except the lateral force, as shown in Figure 2-5. In Kirchhoff–Love plate theory, there are no body forces or tangential forces acting on those directions on membrane, the following equations of equilibrium were obtained for the middle plane

$$\frac{\partial Nx}{\partial x} + \frac{\partial Nxy}{\partial y} = 0$$

$$\frac{\partial Nxy}{\partial x} + \frac{\partial Nx}{\partial y} = 0 \qquad (1)$$

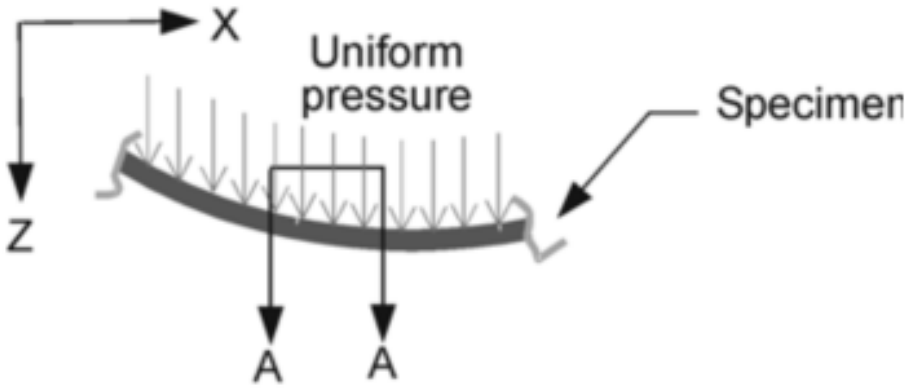

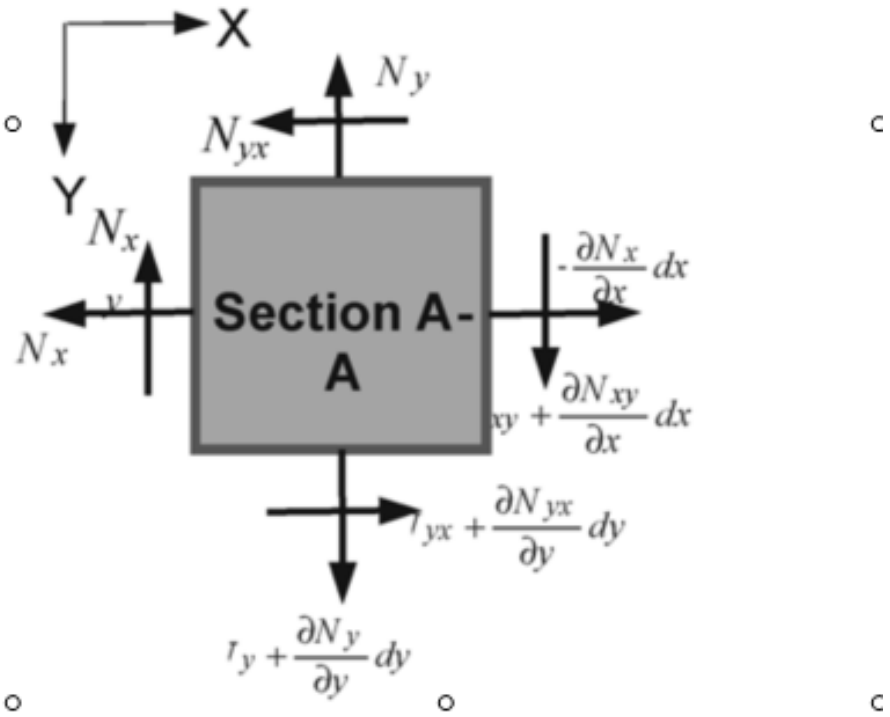

Figure 2-5 Free-body diagram of a small element in the Specimen. [35]

In here, Nx and Ny can be perceived normal forces per unit length. Where Nxy ¼ Nyx are shear forces . Membrane deflection is ŋ load intensity is q. Membrane rigidity is represented by the sign D

$$\frac{\partial^4 ŋ}{\partial x^4} + 2\frac{\partial^4 ŋ}{\partial x^2 \partial y^2} + \frac{\partial^4 ŋ}{\partial y^4} - \frac{q}{D} \qquad (2)$$

Another forces like normal force, shear force, lateral loads are the further factors to consider. Membrane deflection ŋ can be expressed by equation (3).

$$\frac{\partial^4 ŋ}{\partial x^4} + 2\frac{\partial^4 ŋ}{\partial x^2 \partial y^2} + \frac{\partial^4 ŋ}{\partial y^4} - \frac{1}{D}\left(q + N_x\frac{\partial^2 ŋ}{\partial x^2} + N_y\frac{\partial^2 ŋ}{\partial y^2} + 2N_{xy}\frac{\partial^2 ŋ}{\partial x \partial y}\right) \qquad (3)$$

Compare equation (2) and (3), we found middle plane strain is quite large. Where h is the thickness of membrane, E is the Young's modulus, v is Poisson's ratio, r is the radial distance of a point of PDMS membrane. We may found the relationship between membrane deformations, load intensity and radius like below:

$$ŋ - \frac{q}{64D} + (a^2 - r^2)^2$$

$$D = \frac{Eh^3}{12(1-v^2)} \tag{4}$$

The largest deformation at the center of membrane like below:

$$\eta_0 = \eta_{max} = \frac{qa^4}{64D} \tag{5}$$

From above equations, we find out the final air pressure inside the chamber, and based on the properties of elastic membrane, we further determine the bending displacement of the membrane. This allows us to calculate the expected volume change of the container, and in turn derive the predicted pumping flow rate. Based on above analysis, we derived a set of optimized design parameters of the micropump, and calculated its expected performance. NEXGEN simulation should be used to simulate the behavior of the micropump, and the results will be compared with theoretical calculation to verify the design model.

Chapter III Fabrication

The proposed micropump can be fabricated with hybrid process. We used PDMS for mold. PDMS also refers to silicones. The chemical formula for PDMS is CH3[Si(CH3)2O]nSi(CH3)3. (Figure 3-1)

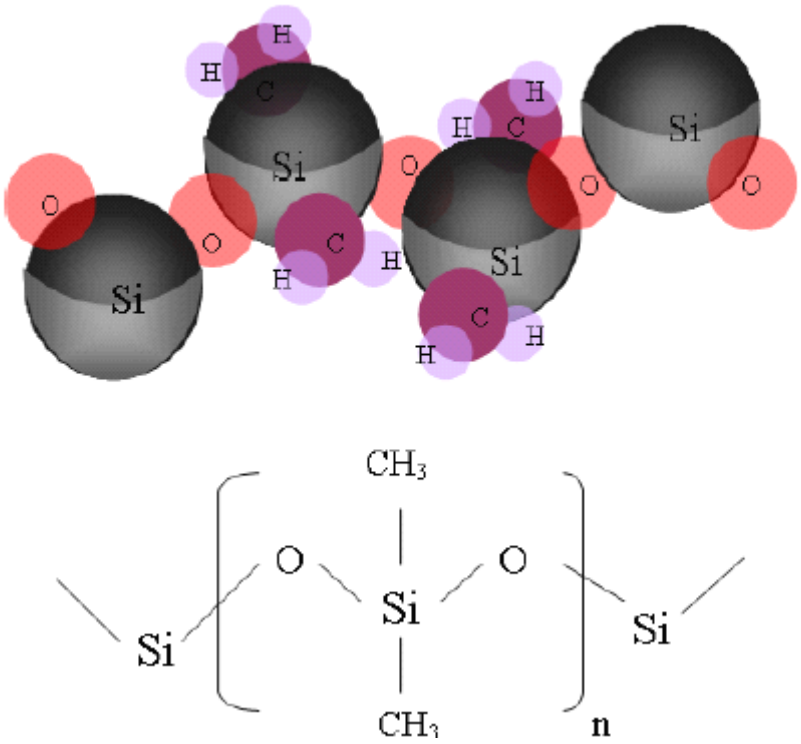

Figure 3-1: chemical formula of PDMS

PDMS has the following advantages [36]

- Non toxic , non flammable Biocompatible
- High chemical inertness
- Clear and transparent
- Gas permeable
- Inexpensive
- Adhesion to metals – applications as inert substrate material

The components are fabricated separately and then assembled together into a micro pump.

1. Fabricate top cover and heating resistor: Starting from Si wafer, deposit 0.4μm Al evaporation [37], and then photolithography and etch Al into thermal resistors. The processes of photolithography will describe in 3.1.

2. Fabricate Si chamber: Starting from silicon wafer, thermal oxidation for 0.6μm SiO_2, photolithography and etching SiO_2 to open etching window. Use Si DRIE (Deep Reactive Ion Etching) [38] to etch down into a chamber. Laser micromachining to drill holes in sidewall [39] and bottom of chamber for inlet and outlet.
3. Assemble components into micropump: Insert elastic membrane into chamber, seal the edge [40], and then bond top cover onto chamber. The micropump is complete.

3.1 Photolithography

Photolithography is using light to transfer a geometric pattern from the sharp we need on the substrate [41]. Simply resist processing, basically consists of six steps (Figure 3-2) [42]

- Substrate clean
- resist coating
- soft baking
- exposure
- development
- Post-development inspection.

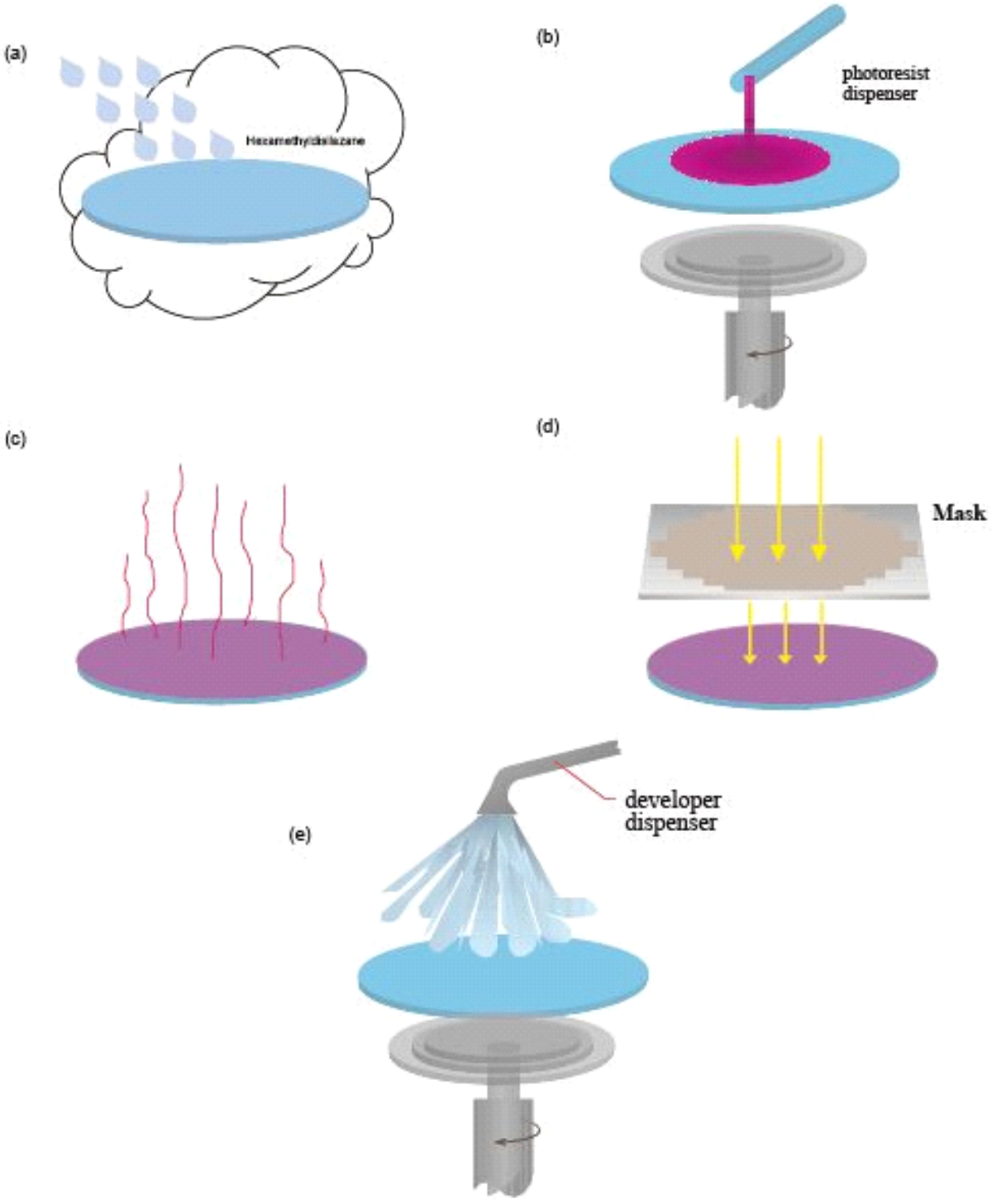

Figure 3-2 Flowchart of photolithography

(a) Substrate clean (b) resist coating (c) soft baking (d) exposure (e) development

3.1.1 Substrate clean

The organic or inorganic contaminations on the surface of wafer after manufacture are inevitable. These residue or particle will affect light blockage and precision. Whole technological process is as follows:

(a). Immerse item in vessel with piranha [43]
Piranha consists of hydrogen Peroxide (H_2O_2) and sulfuric Acid (H_2SO_4). The proportion of the sulfuric acid vs. the hydrogen peroxide is, in this case, 5:1.

(b). The recommended temperature is between 70-100°C. Then use hotplate may for heat the solution. Cleaning time is about 10 to 15minutes.

(c). Remove the wafer from piranha solution to buffered oxide etchant. The main function of it is that clean SiO_2 on the surface.

(d). Wash wafer again by distilled water [44] and dried it out.

3.1.2 Resist coating

Photoresists can be classified into two groups: positive resists and negative resists. When positive exposed to light becomes soluble to the photoresist developer. The negative photoresist is exposed to light become insoluble to the photoresist developer. The unexposed part will dissolve. (Figure 3-3)

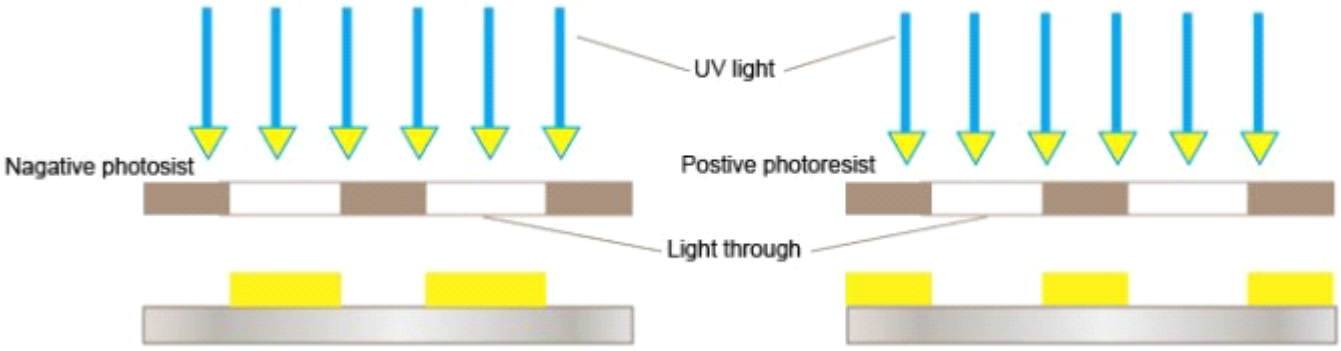

Figure 3-3 Differences PR of photolithographic

Characteristic	Positive	Negative
Adhesion to Silicon	Fair	Excellent
Relative Cost	More Expensive	Less Expensive
Developer Base	Aqueous	Organic
Minimum Feature	0.5 µm and below	± 2 µm
Step Coverage	Better	Lower
Wet Chemical Resistance	Fair	Excellent

Table 3-1 Different between tone types [45]

In this paper we used negative photoresist, because it has larger viscosity. That more easy to make deep sharp. Another reason is less expensive. The step of coating photoresist on wafer is like below:

(1). Put wafer on photoresist coaters.

(2). Use low speed mode [46] []47] that make photoresist distributing equably on wafer surface.

(3). Use high speed mode for ideal thickness.

(4). Keep it on high speed mode for a while for reduce errors. Because the negative photoresist is high viscosity material. When coater stop spinning, photoresist will recover shape .

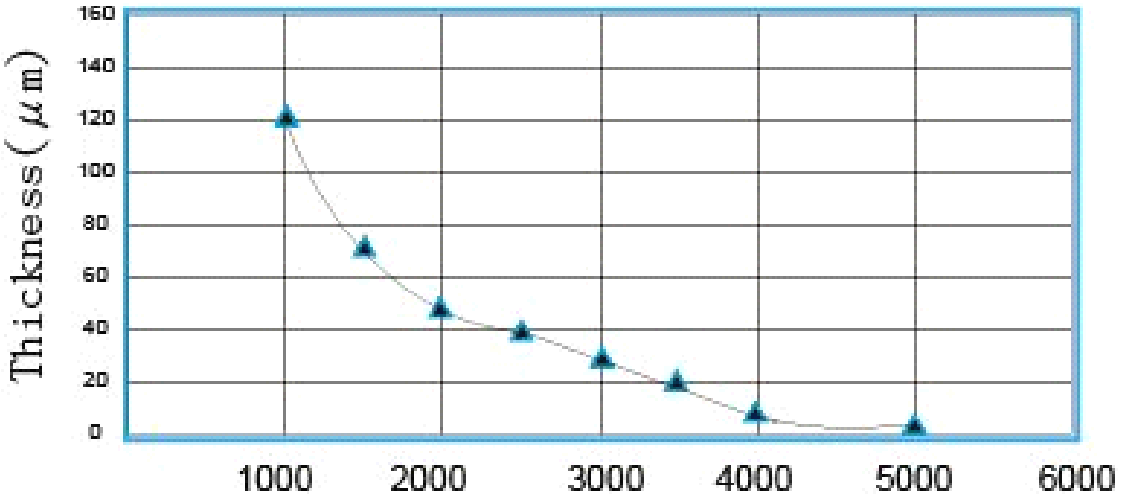

Table 3-2 The relationship between spinning machine and thickness of PDMS

3.1.3 Soft bake:

The next step is followed by the soft bake. First set the hotplate temperature on the appropriate condition. The recommended temperature [48] for soft baking is around 90-100 degree $_oC$. Some situation up to 115$_oC$. Next, place the sample coated with photoresist on the hotplate until the soft baking is over. One of the major purposes of soft bake is that drive away the solvent from wafer. Second reason is that improve the adhesion of the resist to the wafer. The exposure time of soft bake based on the heating methods and the wafer wall in proportion of bake time (wafer wall angel become smaller with shorter bake time).

.

3.1.4 Exposure

Before use photolithography technology, we need to create pattern on mask. Photo mask is opaque plates that allow light to through some holes or transparent part on the plate. The function of photo mask is for defined pattern. Photo mask can roughly divide into two types. First type use laser beam etching pattern on glass or quartz substrate. It has some advantages like high transmittance and lower thermal expansion. That means not easily deformed and more durable. Disadvantages are high production costs and also need many working hours to make it. The second type is printing pattern on plastic film by using high definition printer (10000 dot/ inch). Compare with first type, second one is faster and low costs but lower-resolution because of material characteristic. It fit for device size large than 20 μm. In this poster, the pump size within range. Thus, this paper uses second type (table 3-3).

	Quartz	Glass	Plastic
Minimal size	1~2µm	1~2µm	12.5~20 µm
Manufacturing time	7 days	7 days	2 hous
Cost	High	medium	low

Table 3-3 Differences types of photo mask

3.1.5 Development

Development is the process steps that remove or dissolve the unwanted resist. Development can be immersion developing, spray developing, or puddle developing. Whatever which method, it should be rinsed and dried to ensure that the development action will stop after the developer removed from the wafer surface. The most commonly method is use development solution SU-8 [49].

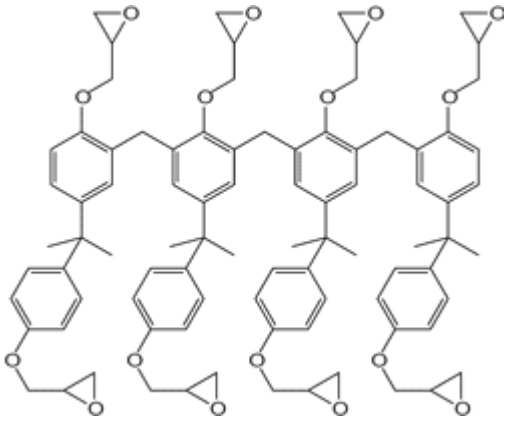

Figure 3-4 SU-8 molecule

3.1.6 Post-development inspection [44]

As the name implies, is an inspection to ensure that get needed result. In normal, it tests by using optical microscope, although SEM and laser-based systems are also used in some post-development inspection tasks. The inspection step checks for contain the following:

- Use of the correct mask
- Resist film quality
- Adequate image definition
- Dimensions of critical features
- Defects and their densities
- Pattern registration.

Chapter IV Result and Discussion

Based on analysis, a set of optimized design parameters of the micropump is achieved, as shown in table 4-1and figure 4-1. FEM Analysis is used to simulate the deformation of the PDMS elastic membrane under given pressure.

Parameter	Dimension
chamber diameter D	2400 μ m
air chamber height h_1	500 μ m
container height h_2	800 μ m
PDMS membrane thickness	40 μ m
young's modulus	**3 Mpa**
Poisson's ratio	**0.49**

Table 4-1 Basic parameter of membrane

In the experiment, we are not only used this parameter for simulation. Because the goal was to find out the best data for this pump. Thus, changed different thickness, size...of membrane is necessary. But didn't change the characteristics of material.

The membrane deflection can be easily to modify by this software. The steps like below:

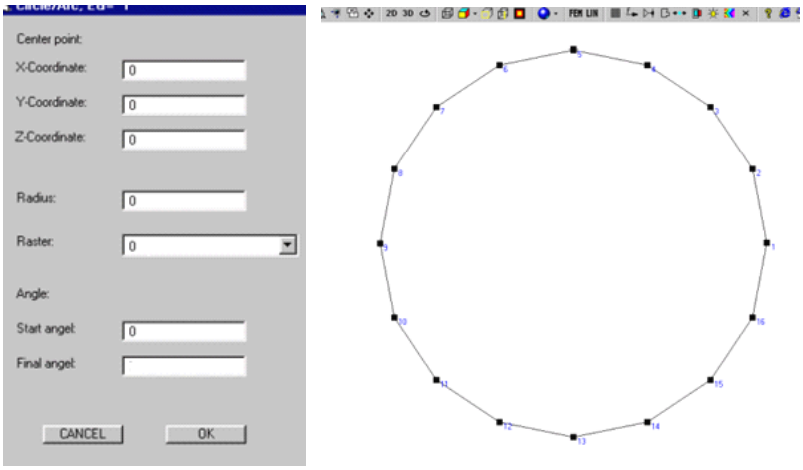

(a.)First, the CAD function could be used for created figure.

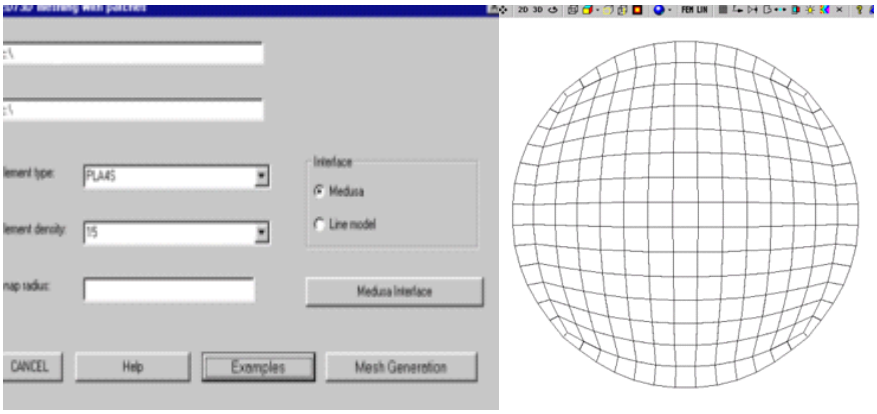

(b) Used meshing tool , also choose model type

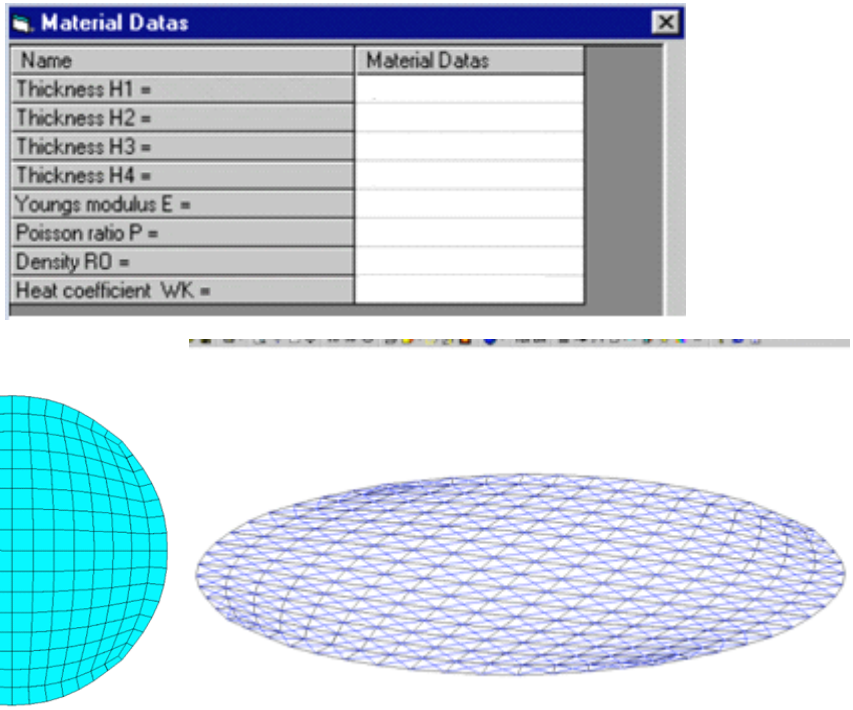

(c) Input elements parameter such like Young's modulus, poisson ratio and density.
Press bottom  that located on tool bar can get 3D figure.

Figure 4-1 (a) (b) (c)Create model by software

In simulation, we increased the pound force per square inch (psi) from 10 psi to 40 psi The maximum deflection is around 250 μm. We knew the maximum deflection, thickness of membrane, diameter of membrane, than we can get radius of curvature. Thus, according to plate theory. This experiment result is close to classical shell theory (h/r < 1/80). Next, we used software to simulate different thickness of membrane and pressure. We found the relationship shown as table 4-2.

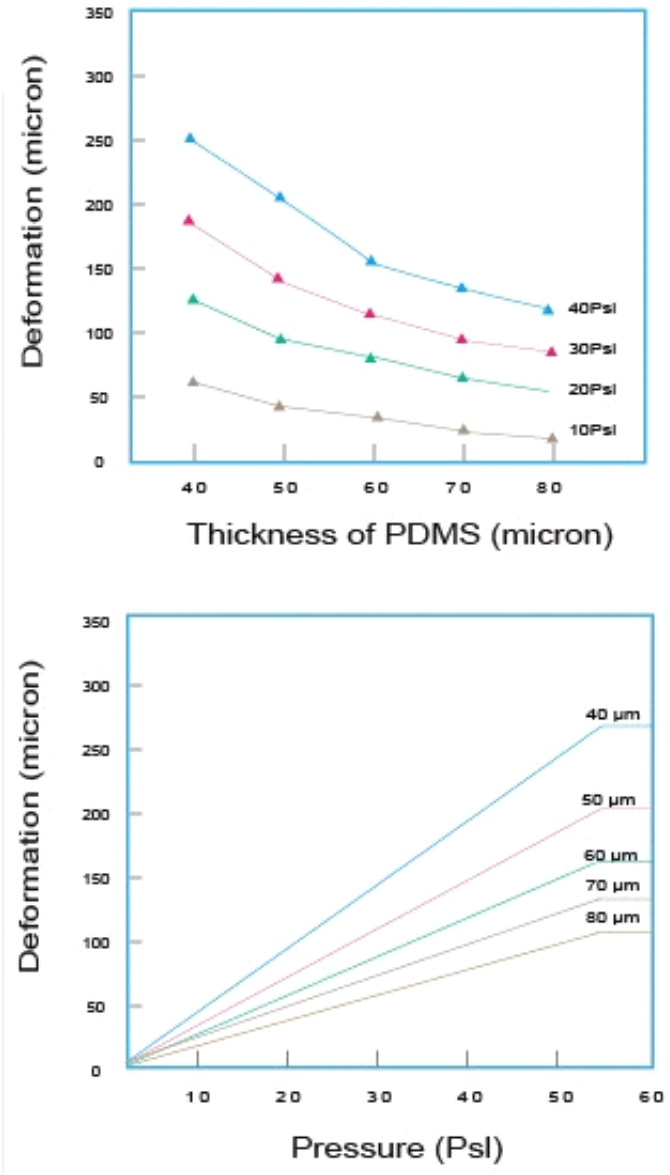

Table 4-2 relationship between deformation and membrane thickness: When membrane getting thicker, deformation become large. The deformation rate directly as the pressure

The maximum deflection is inversely proportional to the thickness. PDMS Membrane is getting thinner and deformation getting large. The top view and side view of the contour plot of the elastic membrane bending shape are shown in Figure 4-2

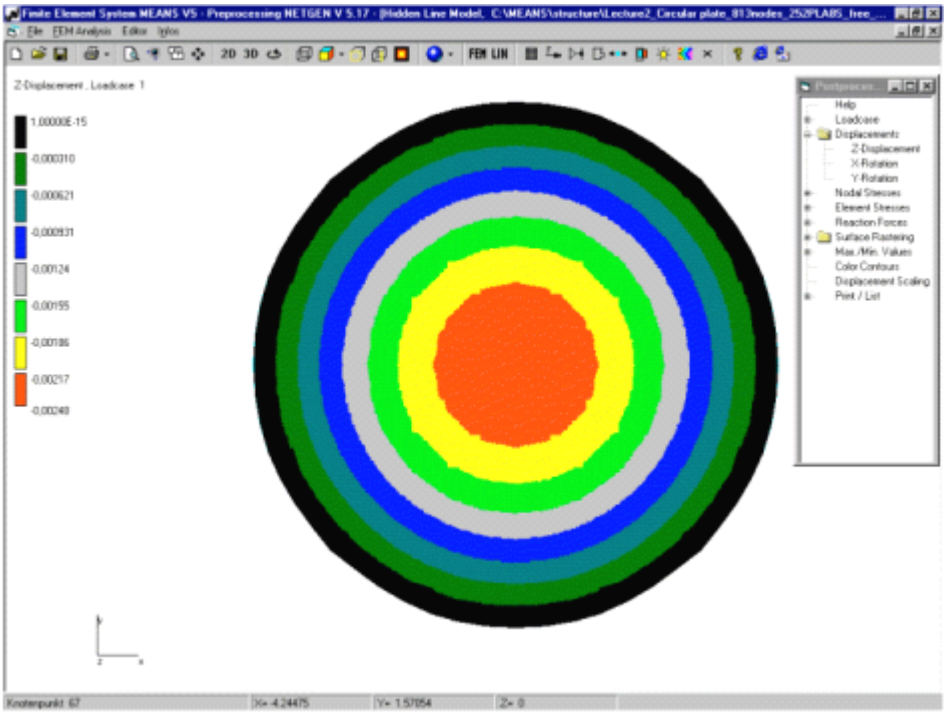

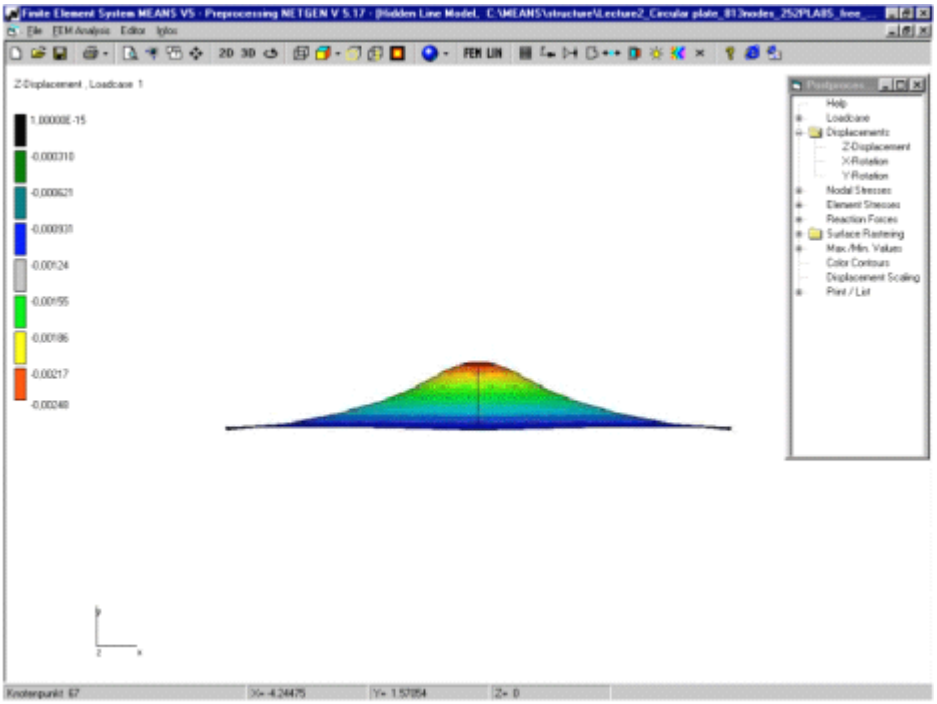

Figure 4-2 Top and side view of pressure on surface

These two figure shows the NETGEN simulation result of the membrane. Different colors mean different displacement. The maximum deflection appeared on the center of diaphragm.

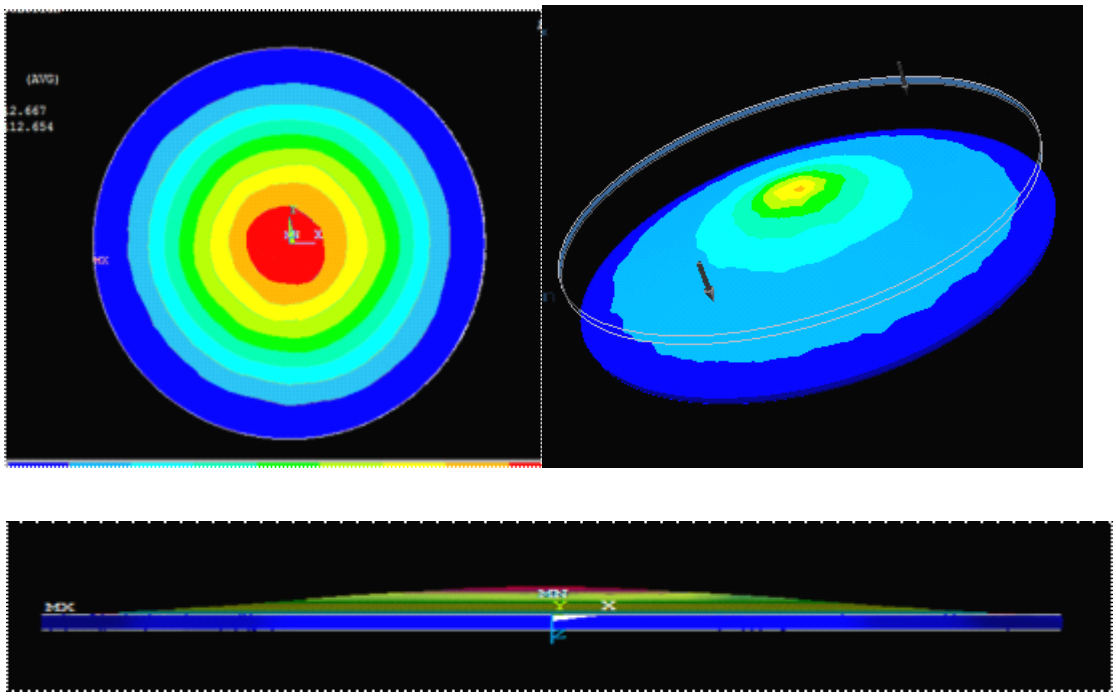

Figure 4-3 Top and side view of pressure on surface

these two figure simulate by Ansys with same parameter like previously pictures. Compare with these two figures, the maximum displacement also occurred on center, but the distance of displacement are slightly different.

The temperature change inside air chamber in response to voltage pulse is shown in table 4-3. As we can see, temperature first increase due to input voltage pulse. Once the voltage pulse is discontinued, the temperature drops quickly due to heat dissipation.

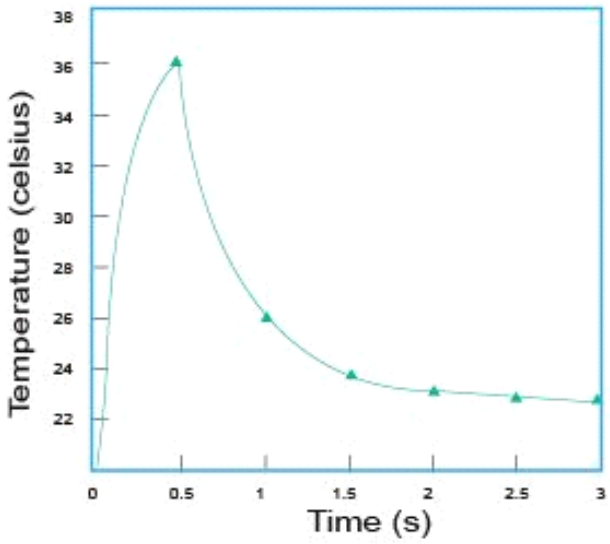

Table 4-3 Relationship between response time and temperature

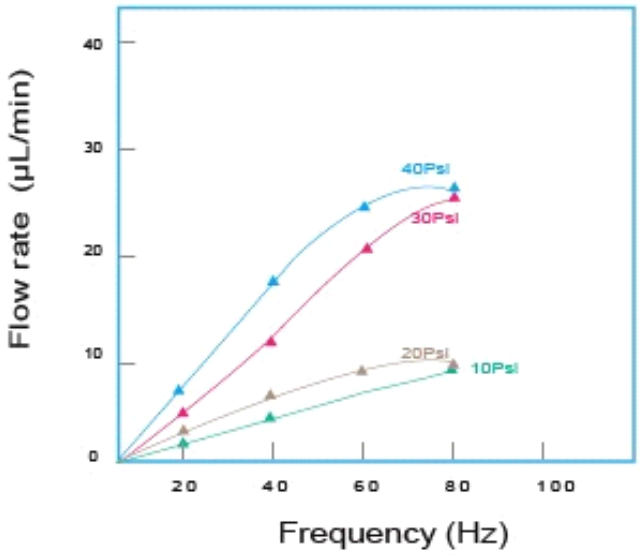

Table 4-4 relationship between frequency and flow rate

In table 4-4, we found the flow rate depend on frequency. We may easy to get flow rate by formula v=ft, f is the frequency of membrane acting, t is average displacement of membrane. Based on the plate theory we know the maximum deflection formula is:

$$\omega = \frac{0.032}{1+\alpha^4}(1-\nu^2)\left(\frac{qb^4}{Eh^3}\right)$$

Bring parameter into this equation we got the maximum deflection of diaphragm based on plate theory. Compare with simulation results. The relationship shown as table 4-5.

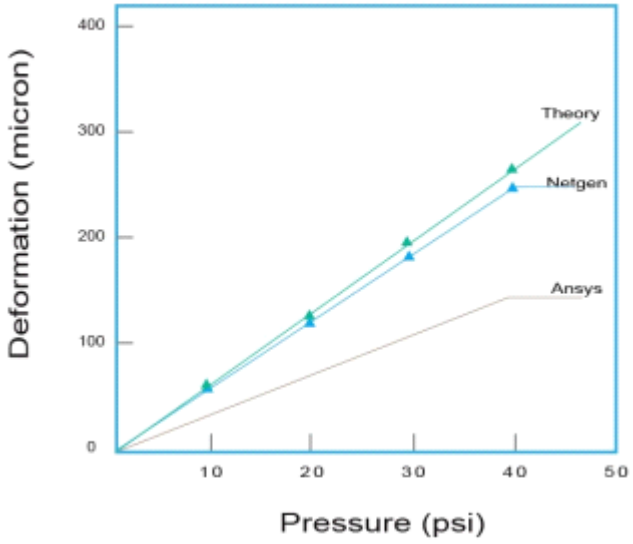

Table 4-5 Simulation and theory results comparison

CHAPTER V Conclusions

In this paper, the design and analysis of a thermal actuated MEMS micropump is proposed. The micropump utilizes air thermal expansion induced by resistor heating to pump microfluid flow. The working principle of the micropump is analyzed. Netgen simulation is used to verify the deflection of elastic membrane with Classical shell theory and first- order shear deformation theory. We found the simulation result are very close to theory. In summary, we found some points:

1. Classical shell theory just considered the straight liner force on plate. This limitation cause it can only use on small displacement calculation. Even-through the pump size is quite small, but we found the process of deflection not only contain straight force. The transverse shear force should be considered and our simulation result also proof this point. First- order shear deformation theory is more closer to real situation than classical shell theory

2. Classical shell theory is a simply way to calculation small displacement with accuracy result. But, based on our simulation result on chapter 4. We found when the membrane thickness larger than 100 μm and displacement more than 20 μm, the transverse shear force should be considered .

3. According to our results, the factors of deflection membrane not only contain Young's modulus, density and Poisson ratio but also considered the wide and thickness of chip or photoresist when it fabricated.. Control the spinning speed of photoresist machine can effect the space between glass substrate and PDMS (chamber wall). Large space size means more thicker of chamber wall in scale and the deflection rate also become large, but also means more difficult for production.

These experimental results data could be provided a prototype of the design pneumatic pump. Now, everything just in computer simulation and only modified the membrane deflection. Only concern the pump body but not included the power controller. In the future, The main job is to make this device more reliable and more reality. Moreover, the further goal is perfectly integration with biochip technology.

CHAPTER XI Acknowledgment

I wish to express my sincere gratitude to principal of University of Bridgeport and prof. Tarek Sobh, Dean of Engineering Department of University of Bridgeport for providing me an opportunity to do my thesis work on "Design and Simulation of a MEMS Thermal Actuated Micropump". This project bears on imprint of many peoples. I sincerely thank to my project director Parbia Patra, Department of Biomedical Engineering and Mechanical Engineering, Xingguo(Michael) Xiong Associate Professor of Electrical and Computer Engineering for guidance and encouragement in carrying out this project work I also wish to express my gratitude to the officials and other staff members of University of Bridgeport who rendered their help during the period of my thesis work. My special thanks to Rhenos LLC company. For their kind co-operation to the completion of my project work. Last but not least I wish to avail myself of this opportunity, express a sense of gratitude and love to my friends and my beloved parents for their manual support, strength, help and for everything

CHAPTER XII References

[1] Lee, Abraham P. and Lee, L. James, " BioMEMS and Biomedical Nanotechnology Vol. 1 Biological and Biomedical Nanotechnology ", United States, 2006

[2] Peter Woias, " Micropumps—past, progress and future prospects ", Science Direct, Vol. 105, no. 1, pp. 28-38, 2005

[3] D J Laser and J G Santiago, "A review of micropumps ", Department of Mechanical Engineering, Stanford University, 2004

[4] Yi-Ning Yang, Fu-Chun Huang and Gwo-Bin Lee,"A New Pneumatic Micropump with a High Pumping Rate and a High Back Pressure," International Conference on Advanced Manufacture (ICAM), Tainan, Taiwan, 2007

[5] Jianhua Tong, Craig A Simmons and Yu Sun, "Precision patterning of PDMS membranes and applications", Journal of Micromechanics and Micro engineering Volume 18 Number 3, 2008

[6] Lynn Khine and Julius M. Tsai, "Design Consideration of Membrane Structure for Thermal Actuated Micropump ", Advanced Materials Research, Volume 254, 2011, pp.42-45

[7] W.Y. Sim, H.J. Yoon, O.C. Jeong, S.S. Yang, A phase change type of micropump with aluminum flap valves, J. Micromech. Microeng. 13 (2003) 286–294.

[8] C.H. Ahn and M.G. Allen, "Fluid Micropumps Based on Rotary Magnetic Actuators", MEMS's 95, 1995, pp. 408-412

[9] C.G.J. Schabmueller, M. Koch, M.E. Mokhtari, A.G.R. Evans, A. Brunnschweiler, H. Sehr, Self-aligning gas/liquid micropump, J. Micromech. Microeng. 12 (2002) 420–424.

[10] K. Junwu, Y. Zhigang, P. Taijiang, C. Guangming, W. Boda, Design and test of a high performance piezoelectric micropump for drug delivery, Sens. Actuators A:

Phys. 121 (2005) 156–161.

[11] V. Lintel et al., " Sensors and Actuators A ", 1988, 15:p. 153-167

[12] W.L. Benard, H. Kahn, A.H. Heuer, M.A. Huff, A titanium–nickel shape memory alloy actuated micropump, in: International Conference on Solid State Sensors and Actuators, vol. 1, 1997, pp. 361–364.

[13] W.L., Benard, et. al., "A Titanium-Nickel Shape-Memory Alloy Actuated Micropump", Proceedings of Transducers'97, vol. 1, pp.361-364

[14] J.W. Judy, T. Tamagawa, D.L. Polla, Surface micromachined micropump, Proc. MEMS 91 (1991) 182–186.

[15] M.M. Teymoori, A.A. Sani, Design and simulation of a novel electrostatic micromachined pump for drug delivery applications, Sens. Actuators A: Phys. 117 (2005) 222–229.

[16] Zengerle, R., et al., "A Hi-Directional Silicon Micropump," Proceedings of MEMS, 1995

[17] C. Zhan, T. Lo, L.P. Liu, A silicon membrane micropump with integrated bimetallic actuator, Chinese J. Electron. 5 (1996) 29–35.

[18] Boehm, S., Olthuis, W., and Bergveld, P., "A Plastic Micropump Constructed with Conventional Techniques and Materials," Sens. Actuators A, Phys., vol. 77, pp. 223-228, 1999.

[19] Manz, A.; Harrison, D.J.; Fettinger, J.C.; Verpoorte, E.; Ludi, H.; Widmer, H.M.; Ciba-Geigy AG, Basel " Integrated electroosmotic pumps and flow manifolds for total chemical analysis systems", Digest of Technical Papers, TRANSDUCERS '91, pp 939-941, 1991

[20] S. Zeng, C.H. Chen, J.C. Mikkelsen, J.G. Santiago, Fabrication and characterization of electroosmotic micropumps, Sens. Actuators B: Chem. 79 (2001) 107–114.

[21] E. Stemme and G. Stemme, "A Valve-less Diffuser/Nozzle based Fluid Pump," *Sensors and Actuators*, vol. A39 (1993) 159-167. E. Stemme and G. Stemme, "Valve-Less Fluid Pump," Swedish Patent Appl. No. 9 300 604-7, 1993

[22] K.S. Yun, I.J. Cho, J.U. Bu, C.J. Kim, E. Yoon, A surface tension driven

micropump for low voltage and low power operations, J. MEMS l.11 (2002) 454–461.

[23] Bruus, H., " Theoretical microfluidics" , Oxford University Press ,2007

[24] Tabeling, P, " Introduction to microfluidics " , Oxford University Press ,2005

[25] P. Karayacoubian, M. M. Yovanovich, J. R. Culham, " Thermal resistance-based bounds for the effective conductivity of composite thermal interface materials ", Department of mechanical engineering, University of Waterloo, Waterloo, Ontario, Canada, pp. 2006

[26] Love, A. E. H, " A Treatise on the mathematical theory of elasticity" , New York: Dover , 1944

[27] Beukema, W.; Limpers, J.; N.V.Philips'Gloeilampenfabrieken, " Resistor dimensions and power dissipation ", Materials and packaging, IEEE Transactions on, Vol.1, USA, January, 2006, pp. 149-157.

[28] Thomson, William, Lord Kelvin ," On an Absolute Thermometric Scale founded on Carnot's Theory of the Motive Power of Heat, and calculated from Regnault's Observations ", Philosophical Magazine,1998

[29] Timoshenko, S. and Woinowsky-Krieger, S., “Theory of plates and shells ", McGraw-Hill New York., 1959

[30] A. E. H. Love, " On the small free vibrations and deformations of elastic shells" , Philosophical trans. of the Royal Society (London), 1888, Vol. série A, N° 17 p. 491–549

[31] R. D. Mindlin ," Influence of rotatory inertia and shear on flexural motions of isotropic, elastic plates ", Journal of Applied Mechanics, 1951, Vol. 18 p. 31–38.

[32] Reddy, J. N., "Theory and analysis of elastic plates and shells" , CRC Press, Taylor and Francis, 2007.:

[33] A. N. Guz' " Generalized theory of shells " , plenum publishing,corporation, 1978.

[34] S. Seren Akavci " The first order shear deformation theory for symmetrically laminated plates on elastic foundations " , Department of Architecture, University of Cukurova Adana, Tyrkey, 2007.

[27] Qiuhua Li, Junghsen Lieh and A Mayer, " Large deflection of laminated circular plates with clamped edge and uniform loading", Proceedings of the Institution of Mechanical Engineers, Part E: Journal of Process Mechanical Engineering, 2005

[35] Lotters, J. C.; Olthuis, W.; Veltink, P. H.; Bergveld, P. " The mechanical properties of the rubber elastic polymer polydimethylsiloxane for sensor applications " , J Micromech Microeng 7 (3): 145–147., 1997.

[36] aguirigan, A. L.; Beebe, D. J, " Integrative Biology" , pp182-195, 2009

[37] Jaeger, Richard C " Film Deposition " , Introduction to microelectronic fabrication.“, 2002

[38] Franz Laermer and Andrea Urban, Robert Bosch Gmbh, “Milestones in deep reactive ion etching”, Transducers’05, 13th international conference on solid state sensors, actuators, microsystems, Seoul, Korea, june 5-9, 2005, p. 1118

[39] C. Rowan," Excimer lasers drill precise holes with higher yields" , Laser Focus World, 1995

[40] Khalid Anwar, Taeheon Han, Sun Min Kim," Reversible sealing techniques for microdevice applications ", Department of mechanical engineering, inha university, 253 younghyun-dong, nam-gu, incheon, republic of Korea , 2010,pp402-751

[41] Jaeger, Richard C, “Lithography". Introduction to Microelectronic Fabrication " , Upper Saddle River: Prentice Hall, 2002

[42] Omkaram Nalamasu, May Cheng, Allen G Timko, Victor Pol, Elsa Reichmanis, Larry F Thompson "An overview of resist processing for deep-UV lithography " , AT&T bell laboratories, Murray Hill,, 1994

[43] "Chemical Specific Information — Piranha Solutions" , Laboratory Safety Manual. Princeton University.

[44] C. Di Bartolomeo, P. Barker, M. C. Petty, P. Adams, A. P. Monkman, " A photolithographic technique for patterning spin-coated polyaniline films ", Advanced Materials for Optics and Electronics, Volume 2, Issue 5, 2004pages 233–236

[45] C. Rowan," Excimer lasers drill precise holes with higher yields”, Boca Raton, Florida: CRC Press. pp. 9, 2002

[46] V.G.Kutchoukov et al., “New photoresist coating method for 3-D structured wafers”, Sensor & Actuator A85, 2000, pp 377-383.

[47] P.Kersten et al., S.Bowstra, J.W.Petersen, “Photolithography on micromachined 3D surfaces using electrodeposited photoresists”, Sensors and actuators , 1995,pp 51-54

[48] Hsu, Jyh-Ping; Lin, Sung-Hwa; Chen, Wen-Chang; Tseng, Shiojenn, " Mathematical analysis of soft baking in photolithography ", Department of chemical engineering, national Taiwan university, Taipei, Taiwan, 2009

[49] John A. Yasaitis, Mary Ann Perez-Maher, Jean Michel Karam, " Thick SU-8 photolithography for BioMEMS micromachining and microfabrication Process Technology”, VIII, 2003

Source code

1: k=1 p=2

```
function main()

    k = 1; % k-th asimuthal number and bessel function
    p = 2; % p-th bessel root

    q=find_pth_bessel_root(k, p);

    N=20; % used for plotting

    % Get a grid
    R1=linspace(0.0, 1.0, N);
    Theta1=linspace(0.0, 2*pi, N);
    [R, Theta]=meshgrid(R1, Theta1);
    X=R.*cos(Theta);
    Y=R.*sin(Theta);

    T=linspace(0.0, 2*pi/q, N); T=T(1:(N-1));

    for iter=1:length(T);

        t = T(iter);
        Z=sin(q*t)*besselj(k, q*R).*cos(k*Theta);

        figure(1); clf;
        surf(X, Y, Z);
        caxis([-1, 1]);
        shading faceted;
        colormap autumn;

        % viewing angle
        view(108, 42);

        axis([-1, 1, -1, 1, -1, 1]);
        axis off;

        H=text(0, -0.3, 1.4, sprintf('(%d, %d) mode', k, p), 'fontsize', 25);
```

```
        file=sprintf('Frame%d.png', 1000+iter);
        disp(sprintf('Saving to %s', file));
        print('-dpng',    '-zbuffer',    '-r100', file);

        pause(0.1);
    end

    % converted to gif with the command
    % convert -antialias -loop 10000 -delay 10    -scale 50% Frame10*
Drum_vibration_mode12.gif

function r = find_pth_bessel_root(k, p)

    % a dummy way of finding the root, just get a small interval where the root is

    X=0.5:0.5:(10*p+1); Y = besselj(k, X);
    [a, b] = find_nthroot(X, Y, p);

    X=a:0.01:b; Y = besselj(k, X);
    [a, b] = find_nthroot(X, Y, 1);

    X=a:0.0001:b; Y = besselj(k, X);
    [a, b] = find_nthroot(X, Y, 1);

    r=(a+b)/2;

function [a, b] = find_nthroot(X, Y, n)

    l=0;

    m=length(X);
    for i=1:(m-1)
        if ( Y(i) >= 0    & Y(i+1) <= 0 ) | ( Y(i) <= 0    & Y(i+1) >= 0 )
            l=l+1;
        end

        if l==n
            a=X(i); b=X(i+1);

            %disp(sprintf('Error in finding the root %0.9g', b-a));
            return;
        end
```

```
    end

    disp('Root not found!');

2 k=0 p=1

function main()

    k = 0; % k-th asimuthal number and bessel function
    p = 1; % p-th bessel root

    q=find_pth_bessel_root(k, p);

    N=20; % used for plotting

    % Get a grid
    R1=linspace(0.0, 1.0, N);
    Theta1=linspace(0.0, 2*pi, N);
    [R, Theta]=meshgrid(R1, Theta1);
    X=R.*cos(Theta);
    Y=R.*sin(Theta);

    T=linspace(0.0, 2*pi/q, N); T=T(1:(N-1));

    for iter=1:length(T);

        t = T(iter);
        Z=sin(q*t)*besselj(k, q*R).*cos(k*Theta);

        figure(1); clf;
        surf(X, Y, Z);
        caxis([-1, 1]);
        shading faceted;
        colormap autumn;

        % viewing angle
        view(108, 42);

        axis([-1, 1, -1, 1, -1, 1]);
        axis off;

        H=text(0, -0.3, 1.4, sprintf('(%d, %d) mode', k, p), 'fontsize', 25);
```

```
        file=sprintf('Frame%d.png', 1000+iter);
        disp(sprintf('Saving to %s', file));
        print('-dpng',    '-zbuffer',    '-r100', file);

        pause(0.1);
    end

    % converted to gif with the command
    % convert -antialias -loop 10000 -delay 10    -scale 50% Frame10*
Drum_vibration_mode01.gif

function r = find_pth_bessel_root(k, p)

    % a dummy way of finding the root, just get a small interval where the root is

    X=0.5:0.5:(10*p+1); Y = besselj(k, X);
    [a, b] = find_nthroot(X, Y, p);

    X=a:0.01:b; Y = besselj(k, X);
    [a, b] = find_nthroot(X, Y, 1);

    X=a:0.0001:b; Y = besselj(k, X);
    [a, b] = find_nthroot(X, Y, 1);

    r=(a+b)/2;

function [a, b] = find_nthroot(X, Y, n)

    l=0;

    m=length(X);
    for i=1:(m-1)
        if ( Y(i) >= 0    & Y(i+1) <= 0 ) | ( Y(i) <= 0    & Y(i+1) >= 0 )
            l=l+1;
        end

        if l==n
            a=X(i); b=X(i+1);

            %disp(sprintf('Error in finding the root %0.9g', b-a));
```

```
            return;
        end
    end

    disp('Root not found!');
```

3 k=0 p=2

```
function main()

    k = 0; % k-th asimuthal number and bessel function
    p = 2; % p-th bessel root

    q=find_pth_bessel_root(k, p);

    N=20; % used for plotting

    % Get a grid
    R1=linspace(0.0, 1.0, N);
    Theta1=linspace(0.0, 2*pi, N);
    [R, Theta]=meshgrid(R1, Theta1);
    X=R.*cos(Theta);
    Y=R.*sin(Theta);

    T=linspace(0.0, 2*pi/q, N); T=T(1:(N-1));

    for iter=1:length(T);

        t = T(iter);
        Z=sin(q*t)*besselj(k, q*R).*cos(k*Theta);

        figure(1); clf;
        surf(X, Y, Z);
        caxis([-1, 1]);
        shading faceted;
        colormap autumn;

        % viewing angle
        view(108, 42);
```

```
        axis([-1, 1, -1, 1, -1, 1]);
        axis off;

        H=text(0, -0.3, 1.4, sprintf('(%d, %d) mode', k, p), 'fontsize', 25);


        file=sprintf('Frame%d.png', 1000+iter);
        disp(sprintf('Saving to %s', file));
        print('-dpng',   '-zbuffer',   '-r100', file);

        pause(0.1);
    end

    % converted to gif with the command
    % convert -antialias -loop 10000 -delay 10    -scale 50% Frame10*
Drum_vibration_mode02.gif

function r = find_pth_bessel_root(k, p)

    % a dummy way of finding the root, just get a small interval where the root is

    X=0.5:0.5:(10*p+1); Y = besselj(k, X);
    [a, b] = find_nthroot(X, Y, p);

    X=a:0.01:b; Y = besselj(k, X);
    [a, b] = find_nthroot(X, Y, 1);

    X=a:0.0001:b; Y = besselj(k, X);
    [a, b] = find_nthroot(X, Y, 1);

    r=(a+b)/2;

function [a, b] = find_nthroot(X, Y, n)

    l=0;

    m=length(X);
    for i=1:(m-1)
        if ( Y(i) >= 0    & Y(i+1) <= 0 ) | ( Y(i) <= 0    & Y(i+1) >= 0 )
            l=l+1;
        end
```

```
    if l==n
        a=X(i); b=X(i+1);

        %disp(sprintf('Error in finding the root %0.9g', b-a));
        return;
    end
end

disp('Root not found!');
```